

Synthesis, Characterization, Functionalization and Bio-Applications of Hydroxyapatite Nanomaterials: An Overview

Muhammad Usman Munir¹, Sajal Salman², Ayehsa Ihsan³, Tilal Elsaman¹

¹Department of Pharmaceutical Chemistry, College of Pharmacy, Jouf University, Sakaka, Aljouf, 72388, Saudi Arabia; ²Faculty of Pharmacy, University of Central Punjab, Lahore, 54000, Pakistan; ³Nanobiotech Group, Industrial Biotechnology Division, National Institute for Biotechnology and Genetic Engineering (NIBGE), Faisalabad, Pakistan

Correspondence: Muhammad Usman Munir, Email mumunir@ju.edu.sa

Abstract: Hydroxyapatite (HA) is similar to natural bone regarding composition, and its structure favors in biomedical applications. Continuous research and progress on HA nanomaterials (HA-NMs) have explored novel fabrication approaches coupled with functionalization and characterization methods. These nanomaterials have a significant role in many biomedical areas like sustained drug and gene delivery, bio-imaging, magnetic resonance, cell separation, and hyperthermia treatment due to their promising biocompatibility. This review highlighted the HA-NMs chemical composition, recent progress in synthesis methods, characterization and surface modification methods, ion-doping, and role in biomedical applications. HA-NMs have a substantial role as drug delivery vehicles, coating material, bone implant, coating, ceramic, and composite materials. Here, we try to summarize an overview of HA-NMs with the provision of future directions.

Keywords: hydroxyapatite nanomaterial, nanoparticle, calcium phosphate, drug delivery system, composite materials, biomimetic

Introduction

Knowledge about the conformation and constitution of natural bone through macroscale to the nanoscale is currently expanding progressively.¹ Previously, the knowledge regarding bone composition and its utilization as a gadget was not explored. Microscopic methods noticeably enhanced bone research, particularly with collagen fibrils, the building blocks of bone.^{2,3} The crystals of bones are the smallest crystals manufactured naturally with 2–4 nm width and a few nm long.⁴ The composition of bone can be ordered in a pyramid fashion, like muscles, with hydroxyapatite (HA) crystals at the pyramid base. Different composition of bone is dependent upon the nature and location of bone in the body. Such compositional arrangement can be either layer-by-layer or lamellar. HA is organized so that c-axes of HA are aligned along the collagen fibril axes.^{5,6} The hierarchical configuration of bone is presented in Figure 1.

HA is chemically defined as the calcium (Ca) apatite in mineral form, whereas apatite is a cluster of minerals having phosphate.⁷ Different salts of calcium phosphate (CaP) are summarized in Table 1. Among several calcium phosphates, HA is the central complex that resembles chemically and conformationally with bone phosphate complexes. Moreover, hydroxyapatite nanomaterial (HA-NM) is a good carrier for the guided release of substances since it is the most stable calcium phosphate derivative.⁸ The scientists observed different conditions relative to pH 6–14, temperature 60–140°C to determine their impact on the HA-NMs structure and shape.⁹ Therefore, HA has various roles in pharmaceuticals, biomedicine, protein chromatography, water treatment, and fertilizers.^{10–12} The characteristics of chemically synthesized HA-NMs are determined by the synthesis method used.¹³ HA is extremely bio-compatible due to its chemical compatibility with biological mineralized bone and is widely used in a range of biomedical applications.¹⁴

HA-NM has great osteoconductive property,¹⁵ and fused with the bone and causes no harmful action. In terms of temperature, pH, and intravascular fluid arrangement, HA-NM is a highly stable calcium phosphate ceramic material.¹⁶ Bioactive and biocompatible properties of HA-NMs make it useful in the biomedical area. It is used mostly in bone tissue-

Graphical Abstract

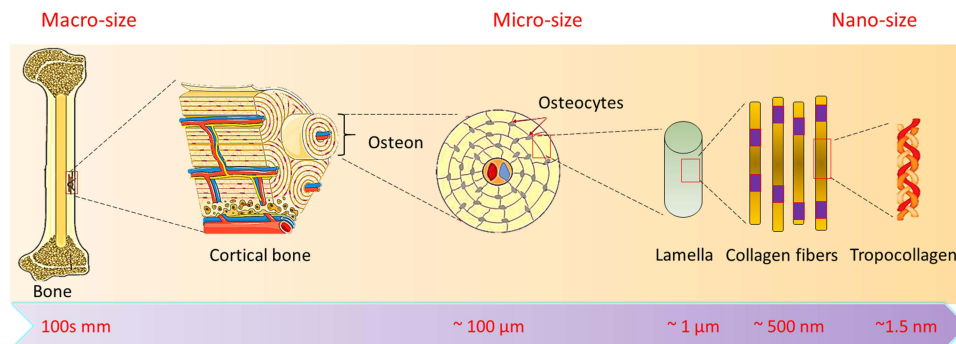
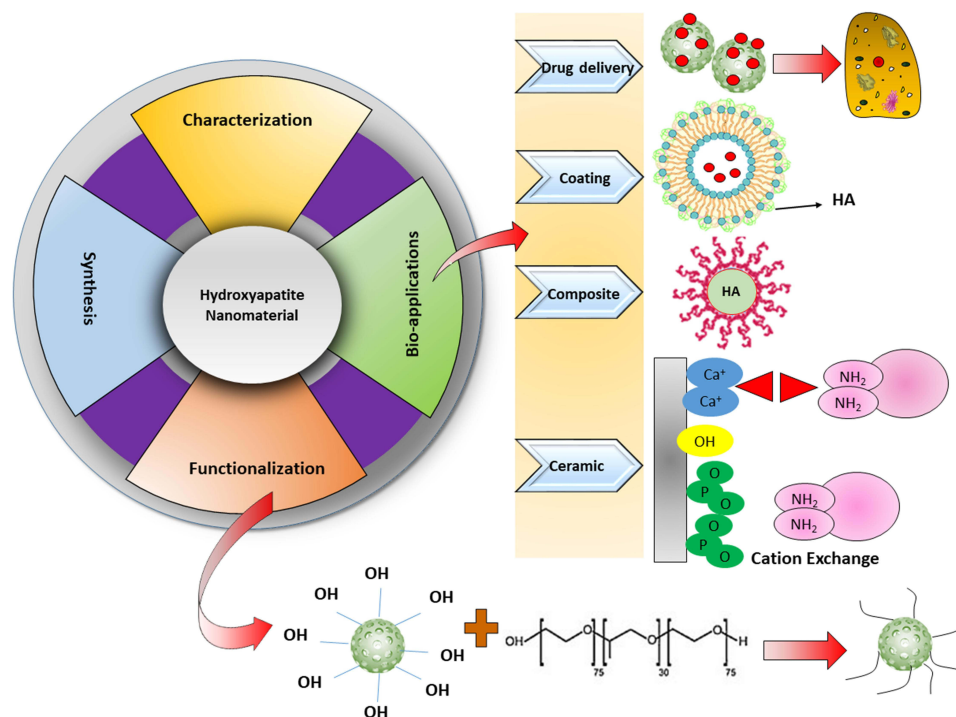


Figure 1 Hierarchical bone configuration at varying size scales. The cortical bone microstructure is made up of osteons with lamellae Haversian channels, while the structural units at the nanoscale are collagen threads having rolls of mineralized collagen fibrils.

regeneration, as reported by several researchers.¹⁷ HA-NM is useful as an implanting substance as well as a coating material. It has also been used as a drug carrier and sustained drug release, which will assist in osteoblastic cell growth.¹⁸ Because of its usefulness in biomedical applications, HA-NM is the topic of research in the field of biomedical research for many years.¹⁹ HAP promotes stiffness in bones and teeth and correlates to the primary component.²⁰ HAP is useful in biological applications because of its physical and chemical similarities to natural enamel. It can be utilized to develop biomaterials based on nanoparticles and nanocomposites, as well as prosthetic bones and teeth.

The scope of this review is to summarize the synthesis strategies and biomedical applications of HA-NMs. Firstly, we discuss the chemical composition, different synthesis methods, and characterization tools for HA-NMs. We classified section two according to the techniques for the synthesis of hydroxyapatite nanomaterials. Secondly, the authors described the surface functionalization of HA-NMs followed by ion-doped HA-NMs. Finally, we detailed the biomedical

Table 1 Different Salts of Calcium Phosphate

| Name | Symbols | Chemical Formula | Ca/P Ratio | Ref. |
|--|---------------|--|------------|--------|
| Tetracalcium phosphate | TTCP | $\text{Ca}_4(\text{PO}_4)_2\text{O}$ | 2.0 | [141] |
| Hydroxyapatite | HA or HAp | $\text{Ca}_{10}(\text{PO}_4)_6(\text{OH})_2$ | 1.67 | [9,10] |
| Fluoroapatite | FA or FAp | $\text{Ca}_{10}(\text{PO}_4)_6\text{F}_2$ | 1.67 | [23] |
| Oxyapatite | OA or OAp | $\text{Ca}_{10}(\text{PO}_4)_6\text{O}$ | 1.67 | [14] |
| Calcium deficient hydroxyapatite | CDHA | $\text{Ca}_{10-x}(\text{HPO}_4)_x(\text{PO}_4)_{6-x}(\text{OH})_{2-x}$ ($0 < x < 1$) | 1.5–1.67 | [5] |
| β -Tricalcium phosphate | β -TCP | $\text{Ca}_3(\text{PO}_4)_2$ | 1.5 | [36] |
| α -Tricalcium phosphate | α -TCP | $\text{Ca}_3(\text{PO}_4)_2$ | 1.5 | [7] |
| Octacalcium phosphate | OCP | $\text{Ca}_8(\text{HPO}_4)_2(\text{PO}_4)_4 \cdot 5\text{H}_2\text{O}$ | 1.33 | [106] |
| Amorphous calcium phosphate | ACP | $\text{Ca}_x(\text{PO}_4)_y \cdot n\text{H}_2\text{O}$ | 1.2–2.2 | [28] |
| Dicalcium phosphate anhydrous (Monetite) | DCPA | CaHPO_4 | 1.0 | [44] |
| Dicalcium phosphate dehydrate (Brushite) | DCPD | $\text{CaHPO}_4 \cdot 2\text{H}_2\text{O}$ | 1.0 | [32] |
| Monocalcium phosphate anhydrous | MCPA | $\text{Ca}(\text{H}_2\text{PO}_4)_2$ | 0.5 | [93] |
| Monocalcium phosphate monohydrate | MCPM | $\text{Ca}(\text{H}_2\text{PO}_4)_2 \cdot \text{H}_2\text{O}$ | 0.5 | [2] |

applications of HA-NMs depending on their use as a drug delivery carrier, coating material, composite material, and ceramic material.

Chemical Constitution and Synthesis of HA Nanomaterials

HA is comprised of calcium and phosphates and is known to be a member of the apatite family. The unit cell formula and general formula of HA are $\text{Ca}_{10}(\text{PO}_4)_6(\text{OH})_2$ and $\text{Ca}_5(\text{PO}_4)_3\text{OH}$, respectively.²¹ The order of calcium and phosphate in the unit cell is such that at M1 and M2 positions, four atoms of calcium are bounded by nine phosphate components, and six calcium atoms are bounded by six atoms of phosphate constituents, respectively. Figure 2 describes the

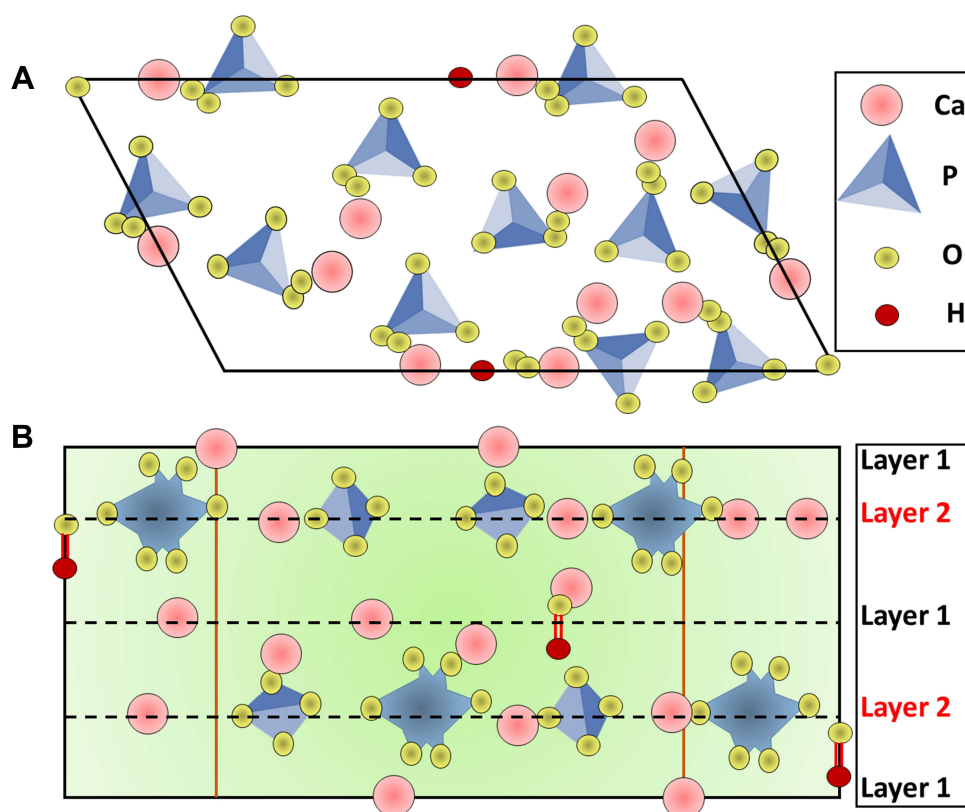


Figure 2 Hydroxyapatite crystal structure, (A) top view and (B) side view. Dashed lines represent one line.

crystallographic structure of hydroxyapatite.^{22–24} Regardless of the original source, HA contains some impurities like hydroxyl ions (OH^-), phosphite ions (PO_3^{3-}), fluoride ions (F^-), and chloride ions (Cl^-). Chloride ions and phosphate ions can change the HA configuration, while hydroxyl ions and fluoride ions can boost the conformational toughness.²⁵

There are numerous methods described for the synthesis of HA-NMs. HA magnitude and arrangement are critically important for their biomedical applications.²⁶ Several reports are available regarding the formation and magnitude of HA-NMs than its arrangement. Electrospinning (ES),²⁷ solid-state (SS),^{28,29} chemical precipitation (CP),³⁰ electrospraying (ESp),³¹ self-propagating combustion (SPC),³² surfactant-assisted precipitation,^{33,34} microwave irradiation (MI),^{35,36} microemulsion (Eme),³⁷ flux cooling (FC),³⁸ and chemical vapor³⁹ are the methods which are known for the synthesis of HA-NMs. Different arrangements (Table 2) and chemical components⁴⁰ result from all these techniques. CP, sol-gel (SG), and hydrothermal are commonly used techniques; however, it is hard to get a high aspect ratio, precise stoichiometry, and high crystallinity. The conventional wet mechano-chemical technique accomplishes stoichiometry of the end product.⁴¹ In these techniques, co-precipitation of $\text{Ca}_3(\text{PO}_4)_2$ and $\text{Ca}(\text{OH})_2$ is performed, followed by conformation purification by calcination at 1000–1200°C. If the stoichiometry of Ca/P is not controlled to 1.67, then the remaining phases like CaO and beta-tricalcium phosphate (TCP) are made at higher and lower values, respectively. Likewise, it is hard to regulate agglomeration, crystal growth, immediate nucleation, and coarsening during the precipitation phenomenon.⁴² Numerous additives such as poly (acrylic acid),⁴³ cetyltrimethylammonium bromide,⁴⁴ allylamine hydrochloride⁴⁵ are applied to prepare the tailored size of the HA-NMs.

The solid-state technique has limited utility due to the long-time duration and requirement of high temperature. It permits the fabrication of different phases of CaP (alpha and beta-TCP). These phases result in adverse changes in the mechanical characteristics of HA, and hence the activity of HA becomes uncertain.⁴⁶ Another method to synthesize HA-NMs is the sol-gel method which has advantages over other methods due to low temperature (less than 400°C) and results in homogeneous nano-sized materials. The precursors in this method, ie, calcium nitrate tetrahydrate ($\text{Ca}(\text{NO}_3)_2 \cdot 4\text{H}_2\text{O}$) and phosphoric pentoxide (P_2O_5) are mixed, frozen, and calcinated at 400–700°C for 8 hr to increase the crystallinity of HA and to remove the impurities.⁴⁷ Quick precipitation technique is prioritized to manufacture uniform nanorods or nanoparticles. This method has supremacy over other methods because it prevents crystal growth as well as nucleation. However, the aging technique can also be utilized for the same purpose.⁴⁸ Besides this, it is hard to get HA-NMs with a high aspect ratio, correct stoichiometry, and sufficient crystallinity.

Techniques for Preparation

The synthesis of HA-NMs is favored across a wide range of compositions, as evidenced by X-ray diffraction patterns that are similar to those of naturally occurring apatite, as seen in the phase diagram of the $\text{CaO-P}_2\text{O}_5\text{-H}_2\text{O}$ system. The gramme atom ratio, Ca/P, was discovered to be in the range of 1.5–2.0 because such a phase is proven to be stable over a vast area in the phase diagram. These findings make it easier to determine the best experimental settings for the creation of HA-NMs. In mildly acidic, neutral, and basic environments, HA-NM is clearly the most stable of the calcium

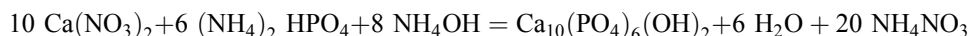
Table 2 Techniques for the Synthesis of Hydroxyapatite Nanomaterials and Their Features

| Method | Symbol | Synthesis Time | Temp (°C) | Size (μm) | Distribution | Shape | Crystallinity | Phase Purity | Cost | Ref. |
|-----------------------------|--------|----------------|------------|-------------|--------------|--------------------|---------------|--------------|----------|---------|
| Core-shell | CS | >24 | 60–120 | > 0.01 | Narrow | Diverse | Variable | Variable | Variable | [10,88] |
| Electrospinning | ES | > 24 | - | 10 × 30 nm | Variable | Fibers | High | Variable | Variable | [21] |
| Self-propagating combustion | SPC | < 24 | 170–500 | > 0.45 | Wide | Diverse | Variable | High | Low | [26] |
| Microemulsion | MEEm | > 24 | RT | > 1 | Narrow | Needle like | Low | Variable | High | [27,31] |
| Microwave irradiation | MI | < 24 | - | 100 × 25 nm | Narrow | Diverse | High | High | Variable | [29,30] |
| Flux cooling | FC | < 24 | 200 | 18 × 2.1 nm | Wide | Hexagonal cylinder | High | Variable | Variable | [32] |
| Chemical precipitation | CP | > 24 | RT | > 0.1 | Variable | Diverse | Low | Variable | Low | [34,35] |
| Hydrothermal | HT | < 24 | 150–400 | > 0.05 | Wide | Needle-like | High | High | High | [40] |
| Electro spraying | ESp | > | - | 75 × 40 nm | Wide | Diverse | Variable | Variable | Low | [42] |
| Solid-state | SS | > | 1150 ± 100 | > 2 | Wide | Diverse | High | Low | Low | [43] |
| Sol-gel | SG | > | 37–85 | > 0.001 | Narrow | Diverse | Variable | Variable | Variable | [44] |

phosphates.⁴⁹ As a result, it is formed by the hydrolysis of other calcium phosphates. Bassett⁵⁰ found that HA-NM precipitates from solutions of calcium oxide and phosphorus pentoxide at acceptable concentrations, which is consistent with the phase diagram's suggestion.

Wet Techniques

The procedures based on precipitation from aqueous solutions⁵¹ are the most suitable for preparing significant quantities of apatite. Because of the ease of experimental processes, high yields, and cleanliness of the samples, a method proposed by Hayek and Stadlman⁵² is commonly employed for this purpose. The approach is based on the equation below.



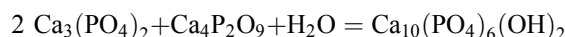
1600 mL of a solution containing 79 g diammonium hydrogen phosphate was dropped under continual stirring into 1200 mL of a solution containing 230 g calcium nitrate, $\text{Ca}(\text{NO}_3)_2 \cdot 4\text{H}_2\text{O}$, which was also kept at the same pH. On the basis of the aforementioned equation, the amounts of reactants taken were meant to provide a yield of roughly 100 g of sample. Based on the dissociation constants of phosphoric acid,⁵³ it can be shown that at the pH maintained, only the orthophosphate ions are dominant, avoiding the expected problems caused by acid phosphate coprecipitation.

By heating the filtered product to around 250°F, the associated volatile ammonium salts were sublimed off. The researchers used this process to generate HA-NM samples for X-ray diffraction and spectrum analyses after making minor modifications. This process was expanded to the synthesis of a few other isomorphs of HA-NMs with appropriate modifications, the main alterations being the complexing of metal ions with acceptable ligands.⁵⁴ Narasaraaju et al updated this process, with the most significant change being the substitution of ethylene diamine for ammonium hydroxide.⁵⁵

Arnold et al⁵⁶ used a simultaneous addition of ammoniacal solutions of calcium acetate and ammonium phosphate to roughly 10 l of a mechanically agitated ammonium acetate solution, which was also kept alkaline, to obtain HA-NM of a high degree of purity. These procedures, which entail precipitating HA at high dilutions, have low yields and are hence inappropriate for preparing large volumes of samples quickly. Through proper modification of the foregoing procedures, the scientists generated samples of HA-NMs that were crystallinity and gramme atom ratio, Ca/P, similar to human tooth enamel. Narasaraaju et al used a judiciously modified method of Hayek and Stadlmann to obtain HA-NM and calcium arsenate apatite, as well as a series of solid solutions, over the entire compositional range, with the method also being successful for the preparation of phosphate and vanadate apatite of lead and arsenate apatite of barium. Several investigators have used the wet procedures described above with slight modifications to generate HA-NMs samples for specialized uses in recent years.⁵⁷

Dry Techniques

It is well known that when a dense heterogeneous mixture of suitable solid ingredients is heated to the right temperature, solid state diffusion of constituent ions can result in the formation of a desired lattice. Tromel looked into the best conditions for forming HA-NMs via a solid-state reaction involving tri and tetra calcium phosphates, or tricalcium phosphate and calcium oxide alternately.⁵⁸ On heating for a few hours at 1050°C in a current of moist air, solid mixes of these materials in proper composition with a gramme atom ratio, Ca/P, equal to 5/3, generated HA, as described by the following equations.



Hydrothermal Methods

As the name implies, hydrothermal procedures⁵⁹ include the application of high temperatures to aqueous solutions in order to enable the precipitation of crystals with dimensions bigger than those obtained using conventional wet methods. Because the boiling point of the aqueous precipitating medium is the upper limiting temperature at atmospheric pressure, heating under high pressure allows this limit to be exceeded. Because the system is subjected to a high temperature in a sealed enclosure, the requisite high pressure is produced by the vapor of the precipitating medium's solvent. The main benefit of such methods has been to improve the crystallinity and purity of the product significantly.

Hayek et al⁶⁰ and Perloff and Posner⁶¹ both obtained similar outcomes, as evidenced by the creation of uniform HA-NMs crystals about 0.1 mm long in the form of hexagonal prisms. 2 g precipitated HA-NM was heated in an autoclave for 24 hours at 380°F with 15 mL 2 M sodium hydroxide solution. The sample's X-ray diffraction pattern included strong peaks, which was expected given its crystal size.

Methods of Characterization

Several characterization methods based on direct visualization or spectroscopy are used for HA-NMs.⁶² The chemical constitution of HA is evaluated by Raman and Fourier transform infrared (FTIR) spectroscopies. These techniques apply distinct properties, which make it easy to estimate the components. For instance, several FTIR peaks of HA have been represented at 574, 602, and 631 cm^{-1} (O-P-O bending), 3572 cm^{-1} (O-H stretching), and 1032, 1046, 1087 cm^{-1} (P-O stretching) (Figure 3A). Whereas Raman spectra peaks are observed at 1045–963 cm^{-1} with tetrahedral PO_4^{3-} and P-O asymmetric stretching peaks are observed at 963 cm^{-1} and 1045–1043 cm^{-1} , respectively. The peaks at these certain points indicate that HA is uniform and extremely crystalline.^{63–65} Elemental composition and details regarding elemental electronic state, empirical formula, and chemical state are studied by X-ray photoelectron spectroscopy (XPS). This method is quantitative spectroscopic and is surface sensitive. Photoelectron signals are displayed by HA-NMs in XPS spectra at 536.1 eV (O 1s), 347.9 eV (Ca 2p), and 133.2 eV (P 2p) (Figure 3B). TOF-SIMS spectra can also confirm the HA-specific peaks shown in Figure 3C.⁶⁶ Lu et al reported that TOF-SIMS spectrum (negative and positive) of CaP are obtained in the range of 0–500 m/z. They observed the prominent intensity peaks of CaO^+ , Ca^+ , and CaOH^+ in the positive spectra, while OH^- , O_2^- , O^- , P^- , HO_2^- , PO_3^- , PO_2^- , and PO^- in the negative spectra. Both these spectra were studied in the range of 1–100 amu. Additionally, impurities of K^+ , Mg^+ , and Na^+ were found in the positive region, and F^- and Cl^- were discovered in the negative spectra.

Munir et al synthesized oval-shaped porous HA-NMs for the delivery of cefazoline in a controlled manner. They reported concentration-dependent high drug loading capacity of HA-NMs due to porous structure and pore volume described by N_2 sorption/desorption and BJH pore volume distribution studies, as shown in Figure 3D–F.⁶⁷ Yang et al explained the HA synthesis mechanism as shown in Figure 4A.⁶⁸ Figure 4B–D is field emission scanning electron microscopy (FE-SEM) images and Figure 4E–G is transmission electron microscopy (TEM) images of CaCO_3 nano-carriers, CaCO_3/HA core/shell, and hmHANPs, respectively. Figure 4D and G are the SEM and TEM images of the final product and present an ellipsoid NP of size 600 nm \times 400 nm having a hollow shape. The porous HA shell is almost 50 nm thick with open windows, responsible for high drug loading. Diffraction peaks at 26.1, 28.45, 30.1, 32.90, 35.97, 40.19, 41.82, 53.56, 55.75, 57.40, 69.12, 74.45, and 77.56, of HA-NMs, analogous to 002, 102, 210, 112, 300, 212, 130, 213, 321, 004, and 104 planes of hexagonal HA unit cell are presented by HA's X-ray diffraction (XRD) profile as shown in Figure 4B.⁶⁹ Details regarding size, morphology, dispersion of the HA-NMs, and shape are studied by direct visualization under FE-SEM, and TEM. The details provided by SEM are incontestable. So, to evaluate the size of the HA-NMs, dispersion, and shape of the HA-NMs, supplementary methods like TEM and atomic force microscopy are utilized. Raman Spectroscopy is also used for confirmation of the hydroxyapatite material, as shown in Figure 4C.

Surface Modifications of HA-NMs

The surface modification of HA-NMs is the method of choice to control the dispersion of HA-NMs, detachment from the composite substances, and then to enable it for a particular use.^{70,71} The most frequent problem faced by the analyst is the aggregation of HA-NMs. Aggregation of nanoformulation is dependent on the reagents and techniques utilized for their synthesis, hydrophilic-hydrophobic interface between the solutions (non-polymeric or polymeric nanoparticles), chemical nature of nanomaterial, and surface energy. Different bridging substances like emulgents and surfactants can be used to address these issues. For instance, researchers utilize bridging substances, ie, hydrostearic acid in poly (L-lactic acid) (PLA) and hydrophilic-hydrophobic HA.⁷² The details of different modifying substances for the hydroxyapatite with respective methods are given in Table 3.

Mediators are the linking substances of amphiphilic nature, and when coated onto the surface of NMs, they help in the stabilization of fine dispersion of NMs.⁷³ However, mediators should not be cytotoxic, interfere with the biological and physiological characteristics of NMs, or affect bioavailability.^{74,75} Various techniques have been utilized for modifying

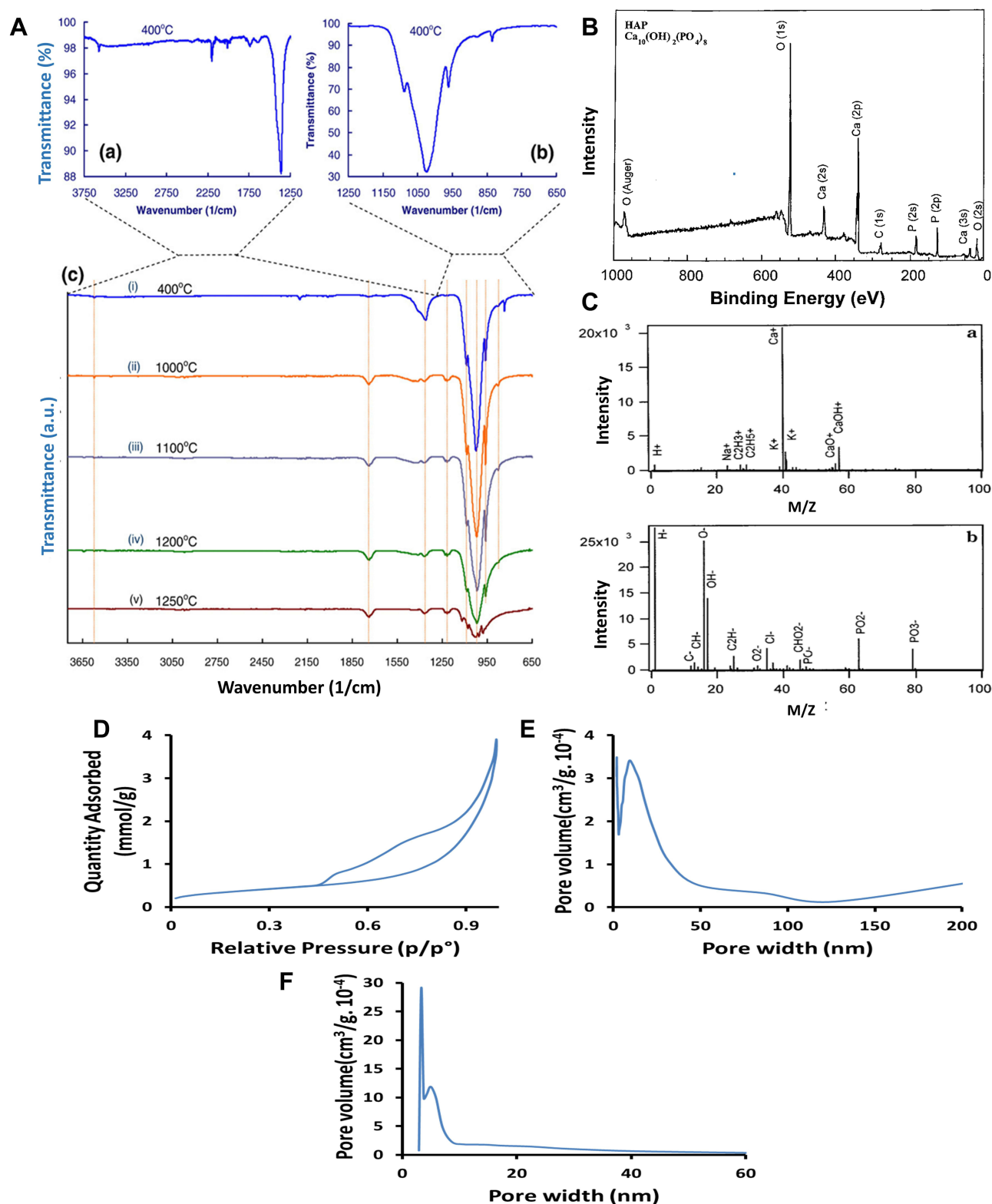


Figure 3 Hydroxyapatite characterization by **(A)** FTIR spectrum of HA-NMs calcined at 400°C (a and b), while (c) signifies IR spectra of HA at different temperature. Figure A reprinted with permission from Elsevier, from: Kalita SJ, Verma S. Nanocrystalline hydroxyapatite bioceramic using microwave radiation: Synthesis and characterization. *Mater Sci Eng C*. 2010;30:295–303.⁶⁵ Copyright © 2010 Elsevier. **(B)** XPS spectrum showing the presence of Ca, O, P with small amounts of contamination (such as C), **(C)** TOF-SIMS spectra (a) Positive and (b) negative. Figures B and C reprinted with permission from American Chemical Society, from: Lu HB, Campbell CT, Graham DJ, Ratner BD. Surface characterization of hydroxyapatite and related calcium phosphates by XPS and TOF-SIMS. *Anal Chem*. 2000;72:2886–2894.⁶⁶ Copyright © 2000 American Chemical Society. **(D)** Nitrogen physisorption isotherms and BJH pore size distribution **(E)** adsorption **(F)** desorption. Figures D-F reprinted with permission from American Chemical Society, from: Munir MU, Ihsan A, Javed I et al. Controllably biodegradable hydroxyapatite nanostructures for cefazolin delivery against antibacterial resistance. *ACS Omega*. 2019;4(4):7524–7532.⁶⁷ Copyright © 2019 American Chemical Society (<https://pubs.acs.org/doi/10.1021/acsomega.9b00541>; further permissions related to the material excerpted should be directed to the ACS).

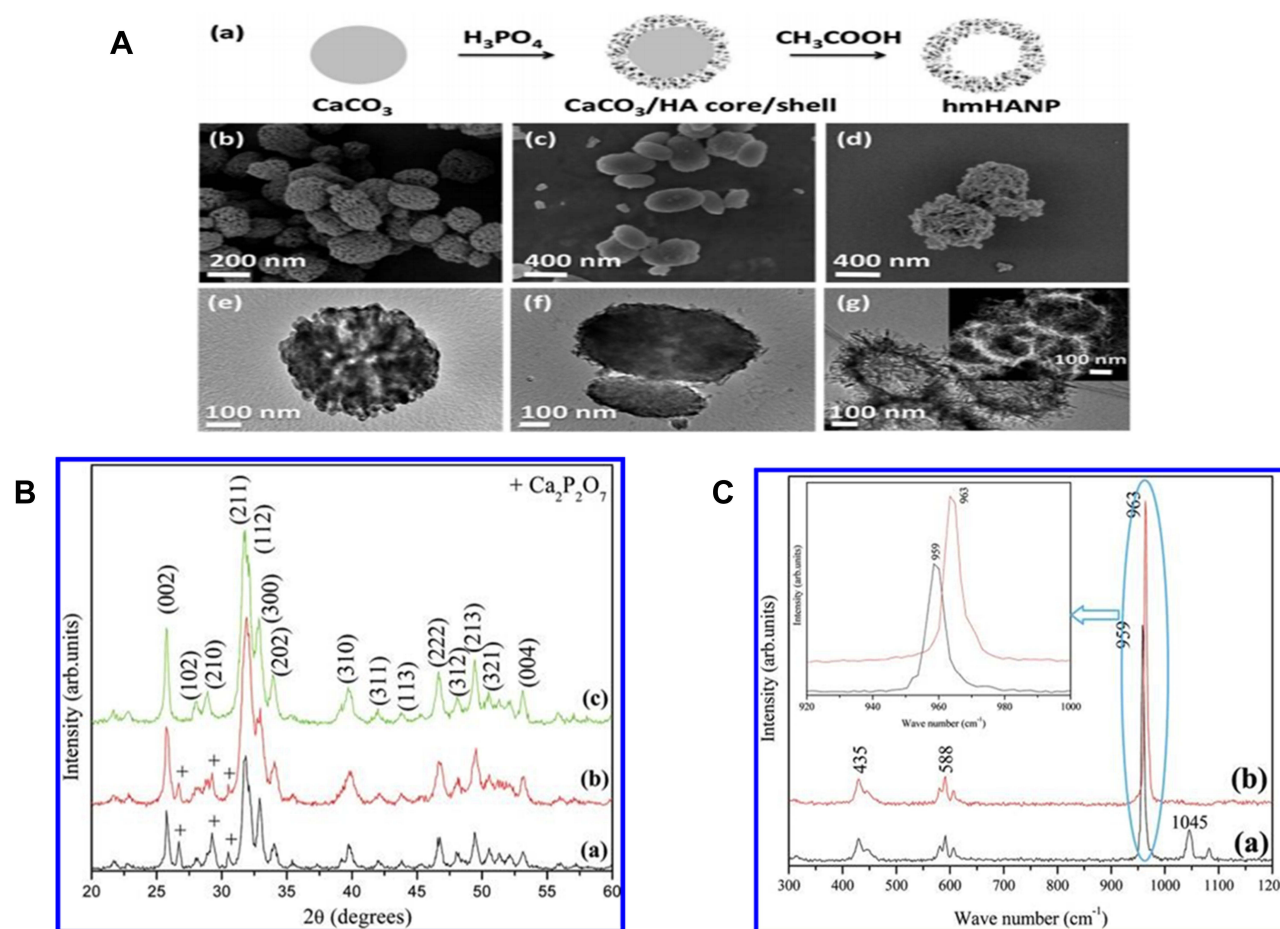


Figure 4 Hydroxyapatite nanomaterials characterization **(A)** (a) An illustration indicating the synthetic process of hollow mesoporous hydroxyapatite nanoparticles (hmHANP). SEM images of (b) CaCO_3 nanoparticles, (c) CaCO_3/HA core/shell nanocomposites, (d) hmHANP; TEM images of (e) CaCO_3 nanoparticles, (f) CaCO_3/HA core/shell nanocomposites, (g) hmHANP (inset: dark-field STEM image). Figure A republished with permission of Royal Society of Chemistry, from: Yang YH, Liu CH, Liang YH, Lin FH, Wu KCW. Hollow mesoporous hydroxyapatite nanoparticles (hmHANPs) with enhanced drug loading and pH-responsive release properties for intracellular drug delivery. *J Mater Chem B*. 2013;1:2447–2450.⁶⁸ copyright © 2013 Royal Society of Chemistry; permission conveyed through Copyright Clearance Center, Inc. **(B)** XRD pattern of HA-NMs synthesized by hydrothermal treatment at 180 °C for (a) 12, (b) 24, and (c) 48 h. **(C)** Raman spectra of nanodisks (a) and nanorings (b). Inset shows the deviation of the specific peak. Figures B and C reprinted with permission from the American Chemical Society, from: Nathanael AJ, Hong SI, Mangalaraj D, Ponpandian N, Chen PC. Template-free growth of novel hydroxyapatite nanorings: formation mechanism and their enhanced functional properties. *Cryst Growth Des*. 2012;12:3565–3574.⁶⁴ Copyright © 2012 American Chemical Society.

the surface. Tanaka et al studied that hexanoic and decanoic acids can alter the HA-NMs surface, as these substances strongly link with P-OH via H-bonding. There are two main advantages of utilizing carboxylic acid. First, animals have different forms of carboxylic acid, eg, vitamins, metabolic inhibitors, fats, and proteins; therefore, the linkage of HA with these moieties is strong. The second advantage is that HA-NMs can be changed from a hydrophilic state to a lipophilic state by utilizing long-chain carboxylic acids.⁷⁶ Tanaka et al further performed the surface alteration by utilizing pyrophosphoric acid (PPA). Treatment of PPA with P-OH part of HA-NMs results in supplementary P-OH moiety coupled with H_3PO_4 .⁷⁷ After PPA treatment, oleic acid and sodium dodecyl sulfate (SDS) were used as biocompatible amphiphile to modify the HA-NMs surface.^{78–80} SDS attached to HA electrostatically, and scientists immobilized the polyvinyl pyrrolidone (PVP, hydrophobic-based interaction of HA-NMs with PVP), and bovine serum albumin (BSA, electrostatically interaction of SDS with HA-NMs) on SDS modified HA-NMs.⁸¹

Inorganic stuff like silanes is also used for surface modification due to linking capability, adhesion stimulation, and talent as mediators for organic and inorganic materials. HA bound silanes are observed to be non-toxic to the cells compared to non-bound HA.^{82,83} Because of this, silanes are applied in the synthesis of materials applicable to bone implantation and dentistry.⁸⁴ Grafting is also an optimal technique for HA-NMs surface modification by using polymers to improve growth factors and dispersion to increase cellular growth. For instance, a study presented the grafting of

Table 3 Various Methods Applied for the Modification of Hydroxyapatite

| Modifying Substance | Method | Ref. | Modifying Substance | Method | Ref. |
|---|-----------------|------|--|----------------|-------|
| Insulin | Grafting | [10] | L-lactide (LA) | Polymerization | [67] |
| BMP-2 | Grafting | [49] | Poly L-lactide (PLLA) | Grafting | [68] |
| Hydro stearic acid | Direct reaction | [54] | Vinylphosphonic acid | Grafting | [69] |
| Decanoic and hexanoic acids | Direct reaction | [57] | Ethylene glycol methacrylate phosphate | Polymerization | [121] |
| Pyrophosphoric acid (PP) | Direct reaction | [59] | Glycidoxy propyltrimethoxy silane | Coating | [67] |
| Oleic acid | Direct reaction | [60] | Polyacrylic acid | Coating | [37] |
| Sodium dodecyl sulphate (SDS) | Direct reaction | [62] | γ-Benzyl-L-glutamate N-carboxy anhydride | Polymerization | [72] |
| Polyvinyl pyrrolidone (PVP) and serum albumin | Grafting | [63] | γ-Methacroyloxy trimethyl silane | Coating | [75] |
| Silanes | Coating | [64] | L-Phenylalanine N-carboxy anhydride | Polymerization | [79] |

L-lactide to HA-NMs via ring-opening polymerization.⁸⁵ In the same report, carbonyl moieties of poly (L-lactide, PLLA) were used to graft PLLA to HA-NMs. It is noted that HA-NMs can be dispersed suitably in PLLA by this technique.⁸⁶

Functionalization with Biological Compounds

Type I collagen, which has molecules that are about 300 nm in length, is the primary ingredient of the bioorganic matrix of bones. Collagen's structural and biochemical properties have been extensively studied, and more than 25 collagen subtypes have been found.⁸⁷ Both human and mammalian bodies include hundreds of different bioorganic chemicals, proteins, and biological macromolecules, in addition to collagens. Because they all appear to be well tolerated by the body, they could be utilized as functionalizing reagents to improve CaPO₄ unique features. CaPO₄ functionalized with gelatin, for example, has been extensively studied as a potential bone replacement biomaterial.⁸⁸ Gelatin foams, for example, have been successfully reinforced with HA and then crosslinked with a carbodiimide derivative. The antibiotic tetracycline was shown to be well carried by such foams. Alginates were also used to functionalize CaPO₄.⁸⁹ Porous HA/alginate formulations based on hydrogels, for example, were generated both biomimetically and by freeze-drying.

Furthermore, chitosan⁹⁰ and chitin⁹¹ functionalization of CaPO₄ is highly common. For example, to functionalize HA powders with chitin, a solution-based approach was established in which the HA particles were uniformly disseminated. Despite the fact that the end products' mechanical characteristics appeared to be poor, microscopic inspections indicated that HA particles had been inserted between the polymer chains, weakening their connections and lowering the overall strength. Similarly, HA functionalized with chitosan was made via a hydrothermal technique from DCPD/chitosan formulations that had already been prepared.⁹² When compared to chitosan alone, the data show that adding CaPO₄ to chitosan improved cell adhesion and produced better cell proliferation and well-spread morphology.

Functionalization of Nano-Dimensional HA-NMs

Researchers frequently face the problem of nanodimensional particle aggregation. It depends on the type of particles, surface energy, reagents and/or procedures employed for synthesis, as well as the hydrophilic/hydrophobic interfaces between the particles and the fluid in the case of suspensions. The surface of nanodimensional CaPO₄ particles must be functionalized to prevent them from aggregating. Different emulsifying agents (such as detergents, coupling agents, and/or surfactants) are employed to accomplish this. To make a stable suspension of nanodimensional HA in chloroform-dissolved polylactic acid, hydrostearic acid was utilised as a surfactant (PLA). The HA powder was efficiently disseminated in hydrostearic acid and homogeneously combined with PLA. As a result, continuous and uniform fibres of HA/PLA formulations were successfully created.⁹³ Similarly, oleic acid was used to functionalize the surface of HA particles in order to distribute them uniformly within poly(ε-caprolactone) matrixes, and lauroyl chloride was used to functionalize biphasic formulations of 90% OCP and 10% HA in order to improve mineral phase dispersion in poly (L-lactic acid) matrices.⁹⁴

Polyacrylic acid was successfully employed to functionalize the surfaces of Eu-doped nanodimensional HA and FA in order to generate stable aqueous suspensions. Stable fluorescent colloids were made using nanodimensional CaPO₄

stabilised by surface functionalization with 5,10,15,20- tetrakis(4-phosphonooxyphenyl)porphine⁹⁵ and oligonucleotides in the same way. Another work successfully functionalized nanodimensional CaPO_4 with the fluorescing dye Cy3.⁹⁶ Additionally, N-(2-aminoethyl)-3-aminopropyltrimethoxysilane was utilised as a functionalizing and dispersing agent to make uniform and stable nanodimensional CaPO_4 particles, which were then loaded with DNA. In addition, the surface of HA particles was functionalized by sorption of decanoic and hexanoic acids to make them hydrophobic and limit their ability to adsorb water and carbon dioxide.⁷⁶

Waterborne polyurethane/HA composites were made by in situ polymerization of functionalized HA to increase mutual interactions between the components. To accomplish so, nanodimensional HA particles were urethanated with 3-isocyanatemethyl-3,5,5-trimethyl-cyclohexylisocyanate to graft isocyanate groups as crosslinkers on their surface, and then polymerized using waterborne polyurethane monomers to generate the required composites. The findings suggested that the functionalized composites could be used to create new biomaterials with superior mechanical, thermal, and water resistance qualities.⁹⁷

Functionalized Nano-Dimensional HA-NMs for Transfection

Functionalized nanodimensional CaPO_4 particles have a wide range of applications, including as carriers of various biomolecules (such as DNA) into living cells to express proteins of interest.⁹⁸ Transfection is the process of purposely putting naked or refined nucleic acids into cells. The word transfection is a combination of trans and infection. Transfection of genetic material (such as supercoiled plasmid DNA or siRNA constructs) or proteins (such as antibodies) is possible. Because many biomolecules are unable to enter live cells on their own, carriers appear to be necessary. The molecules of the transfecting material(s) must either be attached to the surface or incorporated into the bulk of nanodimensional CaPO_4 particles to be transported into the cells. In other words, to be transfected, nanodimensional CaPO_4 particles must be functionalized with a substance.

DNA encapsulation can also be used to functionalize nanodimensional CaPO_4 particles. This was accomplished by dispersing aqueous solutions in hexane in the presence of a surfactant to create microemulsions containing calcium, orthophosphates, and DNA. DNA was encased in the CaPO_4 core and so appeared to be protected from nuclease destruction in those particles. In vitro transfection tests revealed that these carriers had the same transfection effectiveness as the widely available transfecting reagent PolyFect (QIAGEN). Unfortunately, after 24 hours, the particles had become unstable and highly aggregated. Furthermore, nanodimensional CaPO_4 was functionalized with 0.1 wt% positively charged amino acid arginine and 0.3 wt% glucose to increase DNA adsorption. Furthermore, DNA was delivered into *E. coli* and *Staphylococcus aureus* at room temperature using arginine-glucose functionalized CaPO_4 particles, which did not require the preparation of competent cells.⁹⁹

Ion Doped HA-NMs

Researchers are paying attention to the HA-NMs doping with distant ions. However, many studies had been reported about HA-NMs doped ions with less evidence regarding cell culture, making it difficult for analysts to estimate ions doping effect on HA-NMs in association with cells. Several ions are being doped in HA conformation like iron (Fe^{3+}), zinc (Zn^{2+}), silicate (SiO_4^{4-}), strontium (Sr^{2+}), manganese (Mn^{2+}), carbonate (CO_3^{2-}), and magnesium (Mg^{2+}). The details of some are given below.

These doped HA-NMs have an essential role in HA structure as their biochemistry and biological conformation resemble bone.^{100,101} These doped ions cannot alter HA structural conformation as having the compliant ability with many ions. However, sometimes the solubility, crystallinity, and morphology of HA-NMs have been altered. The changes mentioned above cannot affect the properties; although biocompatibility may be changed, as mentioned by Zhao et al. He described that doping ions should be chosen as they may affect the cell properties. In MG63 cells, 1.5 wt% of Mg^{2+} ions cause cell toxicity, but no toxicity for rMSCs case. Equilibrium of negative surface charge also affects the HA-NMs endocytosis and is prominent in MG63 comparative to rMSCs.

Magnesium and Strontium

Sr has a strong affinity for bone, where it is abundant, particularly in areas with high metabolic turnover.¹⁰² Low doses of Sr have long been recognized to be effective in the treatment of osteoporosis, and Sr ranelate administration has recently been shown to lower the incidence of fracture in osteoporotic patients.¹⁰³ Sr ranelate inhibits osteoclast-resorbing activity and osteoclastic differentiation, reducing bone resorption while promoting bone production by boosting pre-osteoblastic cell replication and osteoblastic differentiation. The expanding body of evidence pointing to beneficial outcomes in long-term Sr therapy studies has piqued interest in its integration into HA.

Only Sr-substituted HAs have been tested in vitro on as-prepared materials.¹⁰⁴ The findings of the study, which used osteoblast-like MG63 cells and human osteoclasts, show that Sr has a dose-dependent effect on bone cell behavior. Increased alkaline phosphatase activity, collagen type I, and osteocalcin synthesis all suggest that Sr concentrations in the range 3–7% enhance osteoblast activity and differentiation. Furthermore, even a 1% Sr replacement is enough to impact osteoclast growth, which decreases as Sr content rises.

Cancer cells can be removed by using ion doping, for instance, HA-NMs doped with Mg^{2+} . These materials eliminate the drug toxicity problem, and NMs need conjugating anticancer agents.¹⁰⁵ So, for using HA in cell cultures, the choice of doping ions is very critical. A study observed the outcome of two doping ions, ie, Mg and Sr, on HA-NMs biological characteristics and structural stability. It is noted that negatively charged surface, osteoblast reaction, and density of living cells were enhanced. Moreover, the stability of materials was also improved by Mg and Sr ions presence. It is inferred that mineral metabolism is affected by metal doping ions during the bone remodeling phenomenon. Furthermore, pre-osteoblastic cell proliferation and apoptosis of osteoclasts are boosted. New bone grafting materials can be prepared by doping different ions and are useful in the regeneration of tissue in quick mitigation.¹⁰⁶

Iron and Manganese

In a study, researchers have synthesized Fe^{3+} and Mn^{2+} doped HA-NMs by ion-exchange and wet chemical methods. No morphological and conformational divergence was observed, and the size of the crystal remains the same with single-phase carbonated HA of B-type. Carbonated HA meaning the partial replacement of the carbonate group with phosphates in the lattice conformation. Both doping ions observe no toxic effect on osteoblast cells. Compared to Mn^{2+} doped HA and pristine, HA doped Fe^{+3} showed enhanced negative charge on surface and increased adhesion of osteoblast.¹⁰⁷ Thus, it is indicated that metal ions provide extreme biological and physico-mechanical advantages in tissue engineering. Even high concentrations of these cations are safe, with some exceptions. Likewise, the type of chemical substance used in biomaterials doped with metals must be appropriately selected. Further research is required to determine the action mechanism of doping ions at the cellular level and release pattern from biomaterials. Despite these limits, it is evidenced that metal-doped bio-ceramics have a rapid cure rate and timely applications in the biomedical field.¹⁰⁸

Mn affects bone remodeling regulation, and a deficiency causes a decrease in organic matrix synthesis and a delay in endochondral osteogenesis, increasing the risk of bone abnormalities such decreased bone thickness or length.¹⁰⁹ Mn supplementation has been shown to be an effective inhibitor of bone loss following ovariectomy.¹¹⁰ Mn can substitute for Ca in the structure up to one atom per unit cell (10 at. percent or 5.5 wt. percent) and preferentially enters the M(I) positions, causing a slight rotation of the PO_4^{3-} ion, according to structural analysis of fluoro-apatite synthesized in the presence of Mn^{2+} (ionic radius 0.090 nm) and heat treated at 900°C.

The presence of the Mn^{2+} ion in solution, on the other hand, inhibits HA crystallization and reduces the amount of precipitate.¹¹¹ Furthermore, it was discovered that a high concentration of Mn^{2+} at the surface of HA particles acquired via ion exchange caused a quick drop in HA growth rate in SBF solutions.

Biomedical Applications of HA-NMs

Scientists doing work in biosensors, industry, biomaterials, biochemistry, and bio-mineralization are interested in the association between protein molecules and inorganic substances.¹¹² Generally, NMs have been used for multipurpose especially in combatting antibiotic resistant bacteria.¹¹³ Scholars researching tissue renovation and drug delivery provided enough evidence to evaluate the association between proteins and HA-NMs. Two linking points are present on HA, ie, “P” sites (PO_4^-) and “C” sites (Ca^{2+}), and are different due to their chemical constitution and definite

arrangement. In the crystal lattice, “C” sites are oriented in a rectangular way, while in the hexagonal arrangement are oriented along surfaces of the c-axis.^{112,114} After HA suspension in an aqueous medium, the “C” points are exposed and positively charged. This charge is gained because of OH[−] ions released from the crystal surface and causing Ca²⁺ ion leftovers at “C” site. Consequently, a linkage between protein (negative charge) and Ca²⁺ ions (positive charge) is developed.

A study described that oxygen of −COO ions having negative charge links with HA “C” site.¹¹⁵ Solid-state NMR results have confirmed the interaction between HA surface and −COO[−] amelogenin ions.¹¹⁶ It is stated that negatively charged “P” sites link with positively charged proteins. Furthermore, HA could be utilized in chromatography under physiological conditions to separate proteins of different types.^{117,118} Researchers applied HA-NMs in orthopedics for bone implantation due to their biocompatible characteristics and significant abilities to be utilized in biomedical applications. In addition to HA-NMs, lipid-based NMs are also used to treat bone-relevant diseases, especially rheumatoid arthritis.¹¹⁹

HA-NMs can also be useful in bio-imaging, cancer therapy, and gene delivery, ie, by changing the faulty or missing gene, converting cancerous cells to normal cells, stimulating the elimination of cancerous cells, enhanced regeneration of destructed tissues with prominent growth of new tissues.^{120,121} In fact, it is not easy to apply because of the unavailability of a non-toxic and biocompatible carrier for gene delivery. Researchers revealed that HA-NMs have the ideal properties to carry the gene to be considered a proficient candidate. They differentiated the gene delivery by positively charged zirconia (ZrO₂) and HA, and concluded that gene expression by aqueous HA-NMs is higher in-vitro as compared to ZrO₂.¹²² HA-NMs have provided the emerging role in bio-imaging as suggested by Liu et al, for instance, in imaging intracellular substances and tissues using SiO₂, fluorescein iso-thiocyanate.¹²³ In multifaceted biological measures, organs can be seen by utilizing fluorescence imaging techniques, ie, fluorescent hydroxyapatite (fHA) nanomaterials.¹²⁴

Role as Drug Delivery Carrier

Researchers have been working on using HA-NMs as a potential drug carrier agent for the past two decades and a half.¹²⁵ Munir et al summarized the role of nano HA as a carrier for different drugs like anti-resorptive, anticancer, antibiotics, NSAIDs, and vitamins. They also reviewed the HA role in the delivery of proteins, gene, and radionuclide.¹²⁶ Cellet et al produced HA nanowhiskers to load terbinafine, an antifungal medication, for delivery in the colon, to name a few. The manufactured nanowhiskers [crystallite size of 8.41 nm along (211), and 23.7 nm along (002)] could adsorb about 40.63 mg of terbinafine/g of HA with a BET calculated specific surface area of 67 m²/g. The HA-NMs were found to be good drug delivery vehicles, releasing around 90% of the medication in simulated stomach fluid and approximately 70% in simulated intestinal fluid after 30 hours.

Yu et al¹²⁷ used irregularly shaped HA nanoparticles of 30–40 nm size as carriers of vancomycin hydrochloride to manufacture antibacterial composites to protect prostheses against deep infection (VAN). They did this by incorporating VAN-loaded HA nanoparticles into a sticky matrix of oxidized sodium alginate and gelatin that worked as a good prosthesis adhesive. The loading capacity of HA nanoparticles for VAN was found to be around 956 g per 100 mg of HA nanoparticles. Although the scientists did not investigate the composite’s drug release behavior, the VAN release pattern from bare HA nanoparticles was seen to have two strides. There was a burst release of VAN during the first 24 hours, releasing 61% of the total amount of loaded VAN, and a gradual release of VAN entrapped in HA nanoparticles porosity channels throughout the next 375 hours. The findings clearly show that HA nanoparticles can be used for controlled, long-term medication delivery.

Lian et al,¹²⁸ on the other hand, created a vancomycin-loaded nHA/collagen/PLA bone graft substitute with infection-inhibition properties for mending large-scale bone injury. The composite graft displayed a typical porous structure with a porosity of roughly 80% and compressive strength of 1.52 MPa, despite the shape and size of the utilized HA nanoparticles not being disclosed. The phosphate buffer solution was used to study the release kinetics of VAN from the composite graft in vitro, demonstrating a 98% release of the loaded medication after 4 weeks. The composite graft was found to have a high bacterial inhibition ratio (>99%), strong adherence to the damage site, and no inflammatory reactions when implanted subcutaneously.

Anticancer medications have also been carried by HA nanoparticles. The adsorption and desorption kinetics of drug molecules were seen to be affected by drug characteristics and the shape of HA nanoparticles. The negatively charged alendronate and positively charged cisplatin were substantially adsorbed, whereas the neutral di(ethylenediamine platinum) medronate (DPM) complex had a reduced affinity for HA nanoparticles' negatively charged surface. While cisplatin adsorption was shown to be favored on a needle-shaped HA surface, alendronate adsorption was found to be favored on a plate-shaped HA surface. The rate of release of neutral DPM, on the other hand, appeared to be larger than that of charged alendronate and cisplatin. While neutral DPM released more quickly from needle-shaped HA nanoparticles than from plate-shaped nanoparticles, both charged medications released at similar rates from both types of HA nanoparticles.¹²⁹

HAs-NMs are used as favorable materials in biomedical applications due to their reasonable biocompatibility, non-toxic behavior, suitable carrier talent, structure resemblance with bone, and rough surface.¹³⁰ Many studies demonstrate the role of HA-NMs as a drug vehicle for several drugs confirming their fitness to carry and deliver drugs, as shown in Figure 5.^{10,67,131} The conformation of HA has been modified with spacers like glutamic acid, ie, an amino acid. By applying bifunctional hydrazine bisphosphonate (HBP) with hydrazine linkage, Yewle et al arranged proteins on the HA surface (Figure 6A). The graphs of immobilization of enhanced green fluorescent protein (EGFP) and β -lactamase are presented in Figure 6B and C, respectively. Initially, the surface of HA is modified by HBP, followed by deactivation of the protein by aldehyde functionality. Oxidation of N-terminal of serine and threonine causes aldehyde functionality. Analysts reasoned that organized proteins provide better action comparative to absorbed ones.¹³²

Mesoporous SrHA nanorods and Gd doped luminescent HA are synthesized by Li et al and declared that HA tuned aptamers could be used against cancer cells.¹³³ HA covered by Ti discs is utilized for dexamethasone delivery using biodegradable poly (lactide-co-glycolide) (PLGA) NPs. This document revealed that Ti surface is covered by HA followed by immobilization of dexamethasone-loaded PLGA NPs on the covered Ti.¹³⁴ Mesoporous HA material was synthesized from raw eggshells at room temperature with surface area and pore volume of 284.1 m² g⁻¹ and 1.4 cm³ g⁻¹, respectively. Due to the mesoporous property of HA, increased loading of ibuprofen (1.38 g g⁻¹ HA) was observed coupled with sustained release and reliable dissolution.¹³⁵ Many scientists are working on HA-NMs as drug delivery on implanting material surface and modifying the bio-activity of these materials.^{68,136–138}

Role as a Coating Material

Bone implanting materials could be utilized for treating defective bone as well as for bone remodeling. Various problems occur in synthesizing implanting material like bone repair, the bone coinciding, and implanting substance. The materials used for implantation should be harmless to the immune system. Currently, autografting, synthetic, and allografting

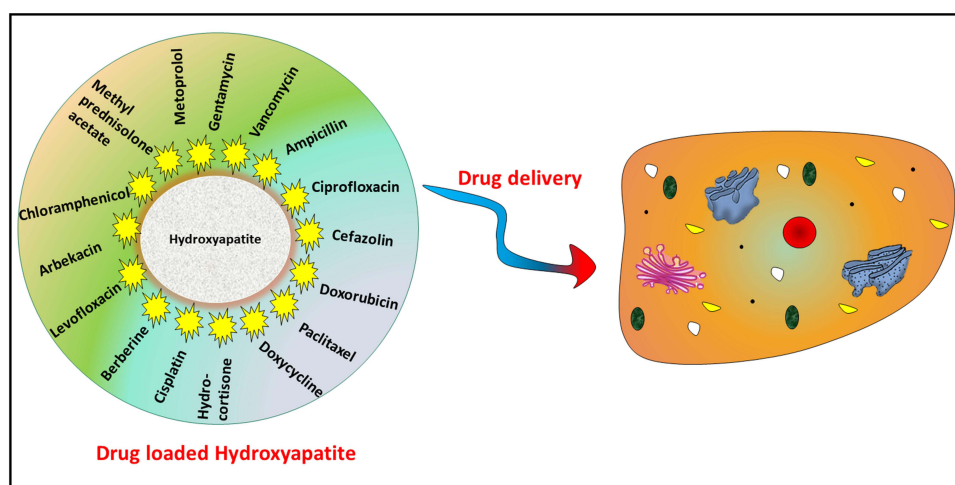


Figure 5 Schematic diagram to express the role of hydroxyapatite nanomaterials in drug delivery.

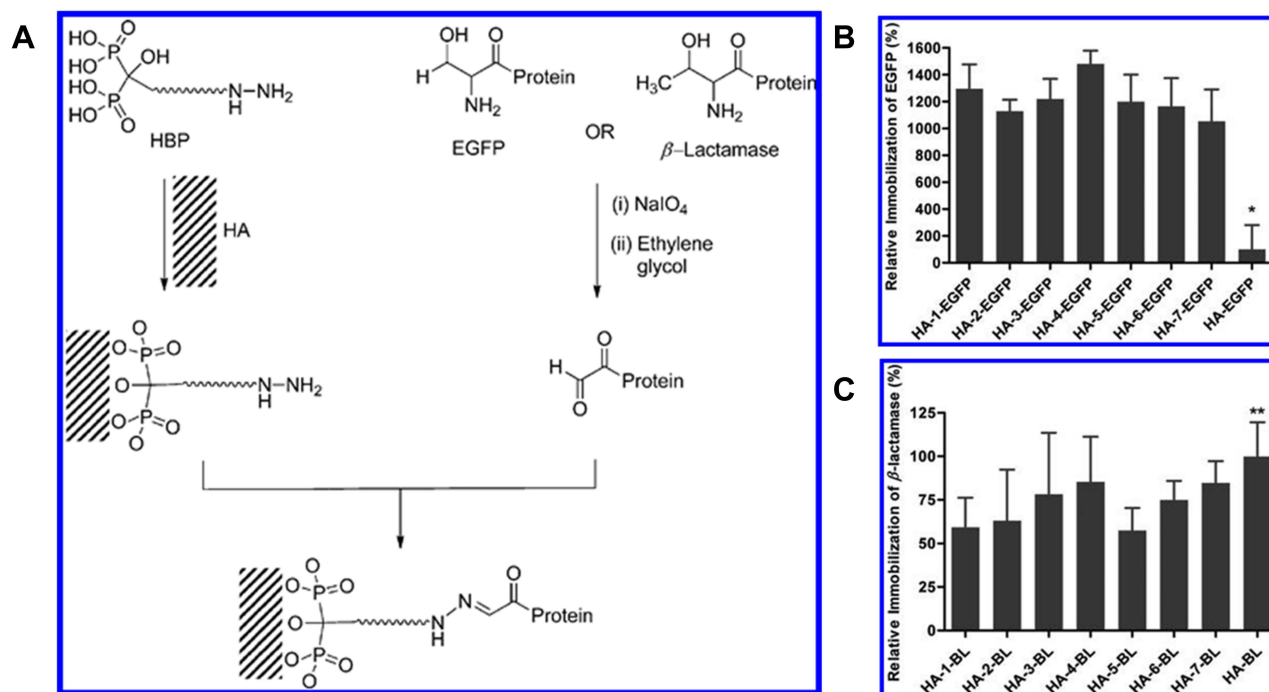


Figure 6 (A) Oriented Immobilization of β -Lactamase and enhanced green fluorescent protein (EGFP) on HA through hydrazine bisphosphonates (HBPs). (B) Immobilization of EGFP and (C) β -lactamase on HA surfaces determined by fluorescence and BCA protein assay, respectively. EGFP and β -lactamase were immobilized on HA surfaces via seven different HBPs (1–7) and by simple adsorption like HA-EGFP and HA-BL, respectively. The corresponding EGFP and β -lactamase are denoted as HA-1-EGFP through HA-7-EGFP and HA-1-BL through HA-7-BL, respectively. HA-EGFP and HA-BL are referred to EGFP and β -lactamase physically adsorbed on HA in the absence of HBP. (* indicates the values are significantly different from others $p < 0.05$, while ** indicates the values are significantly different from HA-1-BL and HA-5-BL $p < 0.05$). Figures A–C reprinted with permission from American Chemical Society from: Yewle JN, Wei Y, Puleo DA, Daunert S, Bachas LG. Oriented immobilization of proteins on hydroxyapatite surface using bifunctional bisphosphonates as linkers. *Biomacromolecules*. 2012;13:1742–1749. ¹³² Copyright © 2012 American Chemical Society.

techniques are utilized for repairing the damaged bone. In synthetic implanting methods, natural bone compliant material or artificially fabricated HA is used; still, there are some restrictions related to these methods. For instance, the material becomes useless due to the absorption of implanting material before bone development.^{139,140} Sometimes, implant infection is caused by the prevalence of the disease, and death may occur, which is truly overwhelming for the community and patient.¹⁴¹ Because of these, it is required to make a new path for implants in bone tissue regeneration. HA-NMs are also used as coating materials for prosthesis bio-integration, as shown in Figure 7A–C. This study has provided three colonization mechanisms anticipated for HA-NMs coatings.¹⁴²

To fabricate the material for implantation, the following characteristics should be kept in mind: Firstly, a morphogenetic signal should be presented by the implant. Secondly, it should possess a signal carrier, thirdly occurrence of excellently vascularized host bed, and lastly, the presence of responsive cells on the implants should be confirmed for the signals.¹⁴³ To increase the action and bioavailability, a method is devised for the coating of bioactive and biocompatible material on the implant. HA is chemically identical to the natural bone applied as a coating substance, and osteointegration increases when the surface of implants is covered with HA.¹⁴⁴ Deterioration is controlled after strong sticking of sintered HA to the bone. Scientists have used the plasma spraying technique to coat HA on Ti implant, and its significance is to prevent sintered-HA fatigue.¹⁴⁵ Pulsed laser deposition, electrostatic sputtering method (layer-by-layer), thermal spraying, solution gel, dip coating, hot isostatic pressing, electrophoretic deposition, hot pressing, and electrostatic spraying are other techniques for HA-NMs coating on implanting material surfaces.¹⁴⁶

Table 3 presents the supremacy and limits of the methods as mentioned earlier. The researchers inferred that the HA-NMs coated Ti alloy has identical sheer power as that of cortical bone.¹⁴⁷ One more study reports the HA-NMs coating on silicon nitride (Si₃N₄) surface, an inert substance, and good mechanical strength. This coating is done to enhance the bioactivity and compatibility, but Si₃N₄ is not used considerably in biomedical science because of inert property.¹⁴⁸ The surfaces coated by HA-NMs can smoothly link with osteoblastic cells, results in the manufacture of osteoids.^{149,150}

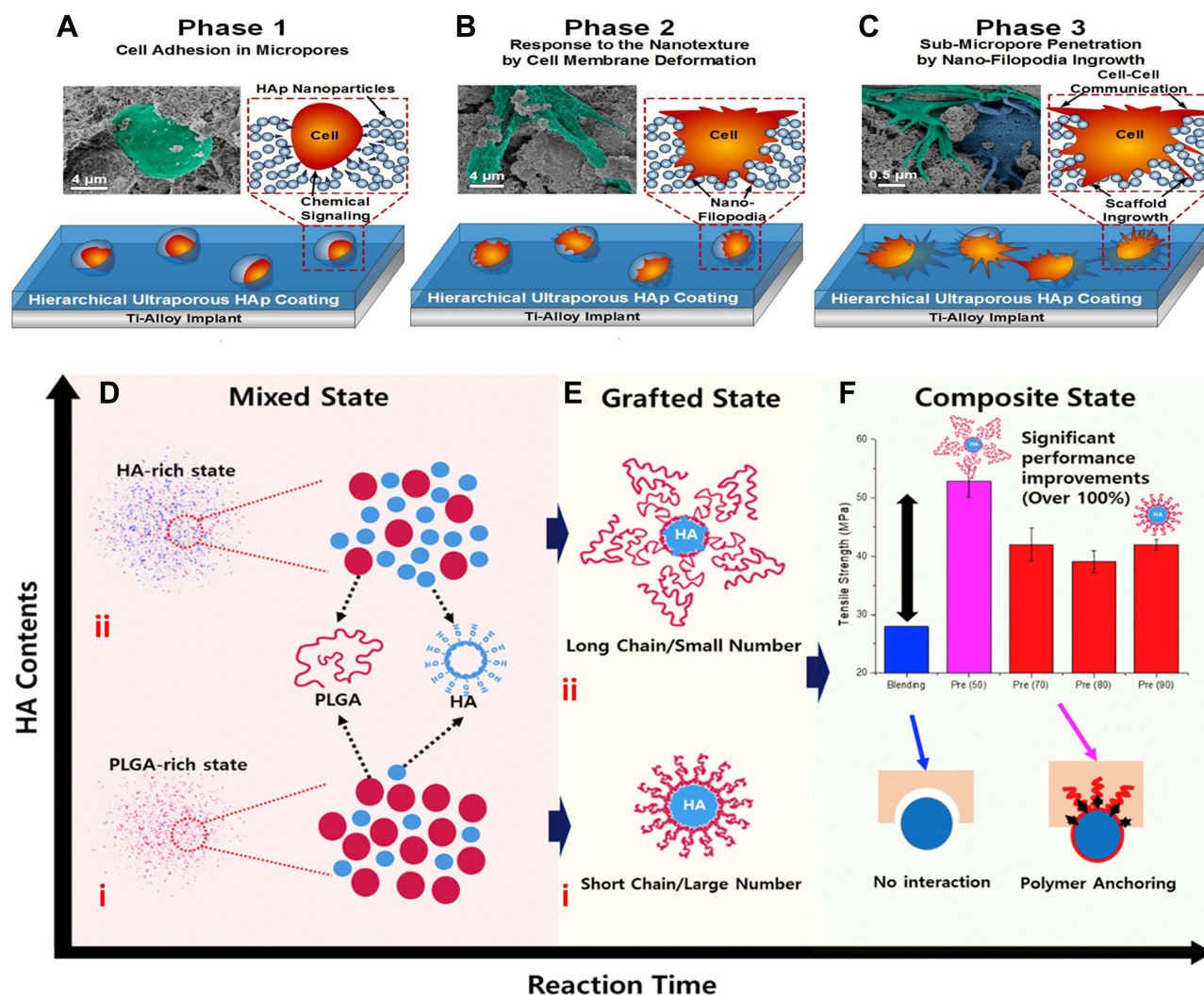


Figure 7 Schematic diagram representing phases of colonization mechanisms anticipated for HA-NMs coating. (A) Adhesion phenomenon starts in the cells by confining anchoring/adhesion spots in micropore surfaces. (B) These cells give response to adjacent hierarchical environment. (C) The growth of filopodia is guided by coating material penetration and resulting formation of nano sized lengthy morphology. Figures A-C reprinted with permission from American Chemical Society from: Nasiri N, Mukherjee S, Panneerselvan A, Nisbet DR, Tricoli A. Optimally hierarchical nanostructured hydroxyapatite coatings for superior prosthesis biointegration. *ACS Appl Mater Interfaces*. 2018;10(29):24840–24849.¹⁴² Copyright © 2018 American Chemical Society. (D) Mixed state including (i) PLGA rich state (ii) HA rich state (E) Grafting state (i) short chain/large number (ii) long chain/small number (F) Tensile strength measurements of PLGA-HA and interaction evaluation of tensile strength with and without PLGA-HA composite. Figures D-F reprinted with permission from Elsevier from: Park JW, Hwang JU, Back JH et al. High strength PLGA/Hydroxyapatite composites with tunable surface structure using PLGA direct grafting method for orthopedic implants. *Compos Part B Eng*. 2019;178:107449.¹⁶⁰ Copyright © 2019 Elsevier.

Researchers observed that osteoinductive characteristics of HA-NMs are also seen when these bind with the bone morphogenetic proteins (BMPs).¹⁵¹ Under desired conditions, the growth of new bone is enhanced by using the methods to coat HA on the implants and metal alloys. The restriction of HA is due to the control of HA coating to survive the physiological load and problems relevant to third-body wear by HA materials.¹⁵²

Role as a Composite Material

In the regeneration of tissues, the use of polymers is considerably and significantly escalating.^{153–155} Polymers may contain natural or synthetic origin with the biodegradable or non-biodegradable property. Researchers assumed the opinion of bone regeneration by using polymers.¹⁵⁶ Likewise, Kulkarni et al inferred that bone tissue regeneration is strengthened by polymer structure-based implanting sites and implants. In long bones, bone regeneration is stimulated by tubular absorbable polymer, and several synthetic polymers are applied either alone or with HA-NMs to enhance the

natural bone matrix.¹⁵⁷ Mostly used polyesters are poly (caprolactone),¹⁵⁸ PLA,¹⁵⁹ and PLGA.¹⁶⁰ Bioactivity and mechanical strength are provided to the composite materials by HA-NMs that act as enforcers.¹⁶¹ PLGA provides high strength to HA-NMs in PLGA/HA composites with the required material surface via direct grafting method, as shown in Figure 7D–F.

It is observed that the research on the uses of HA composite materials is increasing steadily. The regeneration of bone tissue and therapies for bone defects like osteoporosis is advanced by fabricating HA/polymer scaffolds as a vehicle for drug delivery. The researchers reported that polymer itself can be used for efficient drug delivery to cancer cells.¹⁶² HA/PLGA composites are made by integrating PLGA into HA and assumed that accelerated osteogenesis and osteoblastic cell growth are raised after immobility and integration of the proteins with PLGA. Similarly, pamidronic acid is made immobile on HA surfaces to cure osteoporosis. Bones are susceptible to break due to extraordinary osteoclastic action, so according to a report, pamidronic acid lowers osteoclastic action coupled with stimulation of osteoblastic action by HA-NMs.¹⁶³ Scientists fabricated different composites like HA/polyethylene and HA/PLLA for use as bone biomaterials. It is reported that the mechanical power of these composites is enough to be employed in the regeneration of bone.^{164,165}

HA/collagen composite was designed through blending to imitate natural bone, and the bending strength represented by the composite is 5.37 kPa. These composites can be efficiently used for the stability of conformation and finer adhesion. HA/poly (methyl methacrylate) (PMMA) composite is synthesized to play a substrate role for osteoblasts like human cells.^{166–168} Mechanical power and bio-compatibility of minerals based on chitosan are attempted to modify by using different ratios of chitosan and HA-NMs materials. For instance, lyophilization and freezing techniques are used to synthesize HA-NMs and chitosan composites of high molecular weight. High molecular weight chitosan composites have better mechanical characteristics as compared to medium molecular weight chitosan.¹⁶⁹ Several nano HA-collagen configurations are reported having superior biocompatibility and degradation by enzymes.^{170–172}

Role as Ceramics

Natural bone is an example of ceramic composites comprising calcium phosphate, water, and collagen.^{173,174} Besides these components, bone also contains a minor quantity of proteins, polysaccharides, and lipids. Hardness is provided to the bone by calcium phosphate, which is present in HA crystalline form. In addition to bone components, HA consists of some adulterants like F^- , Na^+ , and Mg^{2+} ions and has length and width in nm. HA presence modifies osteoconductive characteristics between the implant and osteoblastic cells and the osteoinductive property of implants.^{175,176} HA is commonly used for bone tissue regeneration either in ceramic, composite, or pristine form is similar to natural bone inorganic cement. The chosen material should be identical to the natural bone for accurate and required consequences. Natural bone is mimicked by fabricating HA bio-ceramics.

Regarding cortical bone, the mechanical strength of the bone and the implant should not be more than factor 55; otherwise, it has a side effect on the bone living cells.¹⁷⁷ Moreover, bone wearing results due to extra rigidity of the implanting material. HA bio-ceramic can be synthesized based on the necessities of the examination and the implanting substance. Zhao et al and Yang et al reported the role of micro/nano HA materials to stimulate osteogenesis of stem cells and trigger angiogenesis and osteogenesis through immunomodulation mechanisms, respectively.^{178,179}

Sintered ceramics have compressive strength, tensile strength, and bending strength of 120–900 Mpa, 300 Mpa, and 38–250 Mpa, respectively. Despite porous ceramics having compressive strength, tensile strength, and bending strength 2–100 Mpa, 3 Mpa, and 2–11 Mpa, respectively, fabricate higher tensile strength implantation material.^{180,181} By scorching the organic substances, the porous ceramics are made with interlinked pores.^{182,183} It is mainly utilized for the growth of bone, its fixation, and drug delivery.^{184,185} Research is continued to synthesize bio-ceramics to mimic the natural bone cement, as shown in Figure 8. Owing to this reason, fibers, metals, nanoparticles, and several strengthening materials are being studied. The biocompatibility of HA has been affected by these substances.

To cope with this problem, Zr bio-ceramic material based on HA is prepared by Ahn et al. It has increased mechanical characteristics and modified the structure to make it more favorable in the dental implanting substance and for orthopedic purposes.¹⁸⁶ Researchers utilized the electrospinning method to manage the conformation of ceramic substances based on HA. By this method, HA crystals are developed on the surface of HA ceramic (negatively charged) in stimulated fluids of

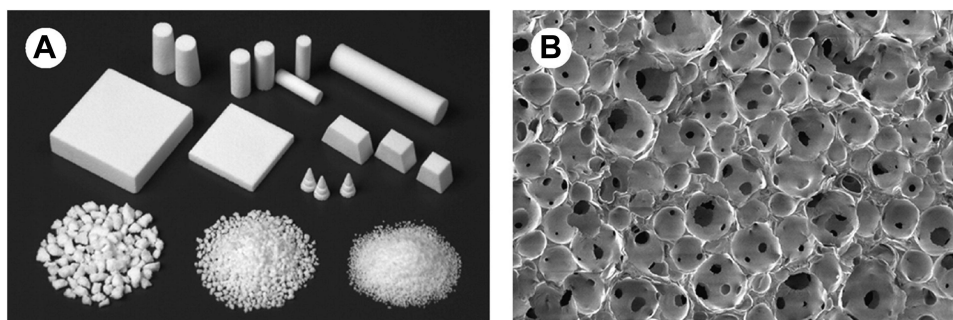


Figure 8 Porous HA ceramics (A) macroscopic image (B) SEM image representing spherical pores of diameter 100–200 μm are unified by pores with diameter 10–80 μm . Republished with permission from The Royal Society from: Yoshikawa H, Tamai N, Murase T, Myoui A. Interconnected porous hydroxyapatite ceramics for bone tissue engineering. *J R Soc Interface*. 2009;6(suppl_3):S341–S348.¹⁹² Copyright © 2009; permission conveyed through Copyright Clearance Center, Inc.

the body.¹⁸⁷ Scientists are trying to make an ideal scaffold to perform the tests on materials like HA/PMMA,^{188,189} HA/collagen,¹⁹⁰ and HA/PLA, and HA/PLGA.^{191,192} Although there are advances in this field, more work is needed to fabricate implanting materials free from infection coupled with increased mechanical power.

Conclusion

In conclusion, we discussed the recent progress in synthesis, characterization, functionalization, and bio-applications of hydroxyapatite nanomaterials. Researchers are doing comprehensive work on HA-NMs due to their resemblance to natural bone regarding composition and structure. Bioactive and biocompatible properties of HA-NMs make them useful in the biomedical area and mostly used in bone tissue-regeneration, as reported by several researchers. HA magnitude and arrangement are critically crucial for their biomedical applications. Scientists for the synthesis of HA-NMs describe numerous methods. Several techniques based on direct visualization or spectroscopy are used to characterize HA-NMs.

For surface modification of HA-NMs, different mediators are applied: the linking substances of amphiphilic nature, and when coated onto the surface of NMs, they help stabilize fine dispersion of NMs. These NMs are used as favorable materials in biomedical applications due to their reasonable biocompatibility, non-toxic behavior, suitable carrier talent, structure resemblance with bone, and rough surface. Bone implanting materials could be utilized for treating the defective bone, and the bone remodeling and HA-NMs work for it. In the regeneration of tissues, uses of HA-NMs and polymers are considerably and significantly escalating, and their combination usage shows significant success in coping with tissue-regeneration-related issues. Bioactivity and mechanical strength are both provided to the composite materials by HA-NMs that acts as an enforcer. HA bio-ceramic can be synthesized based on the necessities of the examination and the implanting substance. Previous reports showed the role of micro/nano HA materials to stimulate osteogenesis of stem cells, and trigger angiogenesis and osteogenesis through immunomodulation mechanism, respectively. In short, HA-NMs are promising nanomaterials with biocompatible and bone similarity features, so they can be used in different biomedical applications.

Sometimes, implant infection is caused by the disease prevalence, and death may occur, which is truly overwhelming for the community and patient. Because of this, it is required to make a new path for implants in bone tissue regeneration. Although there are advances in the role of HA-NMs in ceramics, more work is needed to fabricate implanting materials, which should be free from infection coupled with increased mechanical power.

Future Directions

New materials are made for different purposes with the continuous progress in nanotechnology and materials science.¹⁹³ HA-NMs can be used in drug delivery, orthopedic implant, metallic, and coating implant. About their synthesis methods, it is an open matter to control the morphology and size of HA-NMs uniformly as the previous studies report non-homogeneous and non-uniform formulations. Additionally, textural features of HA-NMs are being controlled by applying a combination of different techniques like the microemulsion method with the hydrothermal technique. Similarly, some

methods have limited utility due to long time duration and high-temperature requirements like the solid-state technique. Thus, new synthesis methods must be discovered to solve these problems.

The aggregation of HA-NMs also provides free space for scientists to work on this topic. Different polymers are used to cope with this problem for a shorter duration but persist and need a permanent solution. Considerable progress reports have given the idea and information about cellular interaction with HA and other ceramics. Usually, HA has no strength to bear the loads; however, scientists are trying to make high mechanical strength material to bear the optimal load. Researchers have used different techniques to link polymers with calcium phosphate and HA, followed by a synthesis of an ideal material with elasticity, toughness, and mechanical power identical to the natural bone. The study should be conducted on the deposition of HA-NMs bio-interactive interface on the polymers (soft and rigid) and their bio-applications. It is suggested that HA-NMs with soft and rigid polymers could be used in skin tissues and bone replacement due to more pliability and superior strength, respectively.

Despite escalating research, many problems are still there for the researchers to avoid the infections. Bone fabrication is increased due to the osteoinductive and osteoconductive properties of HA-NMs. The biological characteristics of HA-NMs are modified by grafting growth factors and fabricating a trustworthy osteoinductive platform. Conversely, limits of HA coatings efficiency at diverse anatomic places, third-body wear by HA-NMs, and ability of HA coating strength to tolerate physiological loads have limited its use. Therefore, additional research work is needed to provide the solutions and further improvement in the biological and mechanical of HA-based implants to ensure their efficacy and safety.

Funding

There was no funding for this work.

Disclosure

The authors declare no conflicts of interest for this work.

References

1. Gu GU, Wu WU, Chen C, Xiao Y. Nanotechnology in the targeted drug delivery for bone diseases and bone regeneration. *Int J Nanomedicine*. 2013;8:2305. doi:10.2147/IJN.S44393
2. Vasilev V, Andreeff I, Sokolov T, Vidinov N. Clinical-morphological and electron-microscopic studies of the growth plate in solitary bone cysts. *Arch Orthop Trauma Surg*. 1987;106:232–237.
3. Nair AK, Gautieri A, Chang S-W, Buehler MJ. Molecular mechanics of mineralized collagen fibrils in bone. *Nat Commun*. 2013;4(1):1–9.
4. Bünger MH, Oxlund H, Hansen TK, et al. Strontium and bone nanostructure in normal and ovariectomized rats investigated by scanning small-angle X-ray scattering. *Calcif Tissue Int*. 2010;86(4):294–306.
5. Fihri A, Len C, Varma RS, Solhy A. Hydroxyapatite: a review of syntheses, structure and applications in heterogeneous catalysis. *Coord Chem Rev*. 2017;347:48–76.
6. Finnilä MAJ, Thevenot J, Aho O, et al. Association between subchondral bone structure and osteoarthritis histopathological grade. *J Orthop Res*. 2017;35:785–792.
7. Szcześ A, Hołysz L, Chibowski E. Synthesis of hydroxyapatite for biomedical applications. *Adv Colloid Interface Sci*. 2017;249:321–330.
8. Chang MC, Ko -C-C, Douglas WH. Conformational change of hydroxyapatite/gelatin nanocomposite by glutaraldehyde. *Biomaterials*. 2003;24:3087–3094.
9. Cao H, Zhang L, Zheng H, Wang Z. Hydroxyapatite nanocrystals for biomedical applications. *J Phys Chem C*. 2010;114:18352–18357.
10. Munir MU, Ihsan A, Sarwar Y, et al. Hollow mesoporous hydroxyapatite nanostructures; smart nanocarriers with high drug loading and controlled releasing features. *Int J Pharm*. 2018;544(1):112–120.
11. Cummings LJ, Snyder MA, Brisack K. Protein chromatography on hydroxyapatite columns. In: *Methods in Enzymology*. Vol. 463. Elsevier; 2009: 387–404.
12. Jiang S-D, Yao Q-Z, Zhou G-T, Fu S-Q. Fabrication of hydroxyapatite hierarchical hollow microspheres and potential application in water treatment. *J Phys Chem C*. 2012;116:4484–4492.
13. Córdova-Udaeta M, Kim Y, Yasukawa K, Kato Y, Fujita T, Dodbiba G. Study on the synthesis of hydroxyapatite under highly alkaline conditions. *Ind Eng Chem Res*. 2021;60(11):4385–4396.
14. Kavasi R-M, Coelho CC, Platania V, Quadros PA, Chatzinikolaïdou M. In vitro biocompatibility assessment of nano-hydroxyapatite. *Nanomaterials*. 2021;11(5):1152.
15. Siswanto S, Hikmawati D, Kulsum U, Rudyardjo DI, Apsari R, Aminatun A. Biocompatibility and osteoconductivity of scaffold porous composite collagen–hydroxyapatite based coral for bone regeneration. *Open Chem*. 2020;18(1):584–590.
16. Kaviya M, Ramakrishnan P, Mohamed SB, et al. Synthesis and characterization of nano-hydroxyapatite/graphene oxide composite materials for medical implant coating applications. *Mater Today Proc*. 2021;36:204–207.
17. Zhou H, Lee J. Nanoscale hydroxyapatite particles for bone tissue engineering. *Acta Biomater*. 2011;7:2769–2781.

18. Koutsopoulos S. Synthesis and characterization of hydroxyapatite crystals: a review study on the analytical methods. *J Biomed Mater Res an off J Soc Biomater Japanese Soc Biomater Aust Soc Biomater Korean Soc Biomater*. 2002;62(4):600–612.
19. Rathia I, Datta P, Balla VK, Nandi SK, Kundu B. Effect of doping in hydroxyapatite as coating material on biomedical implants by plasma spraying method: a review. *Ceram Int*. 2021;47(4):4426–4445.
20. Ghosh S, Ghosh S, Atta AK, Pramanik N. A succinct overview of hydroxyapatite based nanocomposite biomaterials: fabrications, physico-chemical properties and some relevant biomedical applications. *J Bionanosci*. 2018;12(2):143–158.
21. Fadeev IV, Shvorneva LI, Barinov SM, Orlovskii VP. Synthesis and structure of magnesium-substituted hydroxyapatite. *Inorg Mater*. 2003;39:947–950.
22. White TJ, Dong Z. Structural derivation and crystal chemistry of apatites. *Acta Crystallogr Sect B Struct Sci*. 2003;59:1–16.
23. De Leeuw NH. Local ordering of hydroxy groups in hydroxyapatite. *Chem Commun*. 2001;3:1646–1647.
24. Ri M-H, Jang Y-M, Ri U-S, Yu C-J, Kim K-I, Kim S-U. Ab initio investigation of adsorption characteristics of bisphosphonates on hydroxyapatite (001) surface. *J Mater Sci*. 2018;53:4252–4261.
25. Resende NS, Nele M, Salim VMM. Effects of anion substitution on the acid properties of hydroxyapatite. *Thermochim Acta*. 2006;451:16–21.
26. Xu S, Long J, Sim L, Diong CH, Ostrikov K. RF plasma sputtering deposition of hydroxyapatite bioceramics: synthesis, performance, and biocompatibility. *Plasma Process Polym*. 2005;2:373–390.
27. Wu Y, Hench LL, Du J, Choy K, Guo J. Preparation of hydroxyapatite fibers by electrospinning technique. *J Am Ceram Soc*. 2004;87:1988–1991.
28. Ignjatovic N, Suljovrujic E, Budinski-Simendic J, Krakovsky I, Uskokovic D. Evaluation of hot-pressed hydroxyapatite/poly-L-lactide composite biomaterial characteristics. *J Biomed Mater Res Part B Appl Biomater an off J Soc Biomater Japanese Soc Biomater Aust Soc Biomater Korean Soc Biomater*. 2004;71:284–294.
29. Wei M, Evans J. Synthesis and characterisation of hydroxyapatite and fluorapatite. *Key Eng Mater*. 2002;218:35–38.
30. Monmaturoj N. Nano-size hydroxyapatite powders preparation by wet-chemical precipitation route. *J Met Mater Miner*. 2008;18(1):35.
31. Zhang Y, Venugopal JR, El-Turki A, Ramakrishna S, Su B, Lim CT. Electrospun biomimetic nanocomposite nanofibers of hydroxyapatite/chitosan for bone tissue engineering. *Biomaterials*. 2008;29:4314–4322.
32. Tas AC. Combustion synthesis of calcium phosphate bioceramic powders. *J Eur Ceram Soc*. 2000;20:2389–2394.
33. Bose S, Saha SK. Synthesis and characterization of hydroxyapatite nanopowders by emulsion technique. *Chem Mater*. 2003;15:4464–4469.
34. Sarda S, Heughebaert M, Lebugle A. Influence of the type of surfactant on the formation of calcium phosphate in organized molecular systems. *Chem Mater*. 1999;11:2722–2727.
35. Lak A, Mazloumi M, Mohajerani MS, et al. Rapid formation of mono-dispersed hydroxyapatite nanorods with narrow-size distribution via microwave irradiation. *J Am Ceram Soc*. 2008;91:3580–3584.
36. Liu J, Li K, Wang H, Zhu M, Yan H. Rapid formation of hydroxyapatite nanostructures by microwave irradiation. *Chem Phys Lett*. 2004;396:429–432.
37. Koumoulidis GC, Katsoulidis AP, Ladavos AK, et al. Preparation of hydroxyapatite via microemulsion route. *J Colloid Interface Sci*. 2003;259:254–260.
38. Teshima K, Lee S, Sakurai M, et al. Well-formed one-dimensional hydroxyapatite crystals grown by an environmentally friendly flux method. *Cryst Growth Des*. 2009;9:2937–2940.
39. Piccirillo C, Denis CJ, Pullar RC, et al. Aerosol assisted chemical vapour deposition of hydroxyapatite-embedded titanium dioxide composite thin films. *J Photochem Photobiol a Chem*. 2017;332:45–53.
40. Madhumathi K, Shalumon KT, Rani VVD, et al. Wet chemical synthesis of chitosan hydrogel–hydroxyapatite composite membranes for tissue engineering applications. *Int J Biol Macromol*. 2009;45:12–15.
41. Abidi SSA, Murtaza Q. Synthesis and characterization of nano-hydroxyapatite powder using wet chemical precipitation reaction. *J Mater Sci Technol*. 2014;30:307–310.
42. Wu VM, Tang S, Uskoković V. Calcium phosphate nanoparticles as intrinsic inorganic antimicrobials: the antibacterial effect. *ACS Appl Mater Interfaces*. 2018;10:34013–34028.
43. Perkin KK, Turner JL, Wooley KL, Mann S. Fabrication of hybrid nanocapsules by calcium phosphate mineralization of shell cross-linked polymer micelles and nanocages. *Nano Lett*. 2005;5:1457–1461.
44. Cai Y, Liu Y, Yan W, et al. Role of hydroxyapatite nanoparticle size in bone cell proliferation. *J Mater Chem*. 2007;17:3780–3787.
45. Shchukin DG, Radtchenko IL, Sukhorukov GB. Synthesis of nanosized magnetic ferrite particles inside hollow polyelectrolyte capsules. *J Phys Chem B*. 2003;107:86–90.
46. Pramanik S, Agarwal AK, Rai KN, Garg A. Development of high strength hydroxyapatite by solid-state-sintering process. *Ceram Int*. 2007;33:419–426.
47. Agrawal K, Singh G, Puri D, Prakash S. Synthesis and characterization of hydroxyapatite powder by sol-gel method for biomedical application. *J Miner Mater Charact Eng*. 2011;10:727–734.
48. Chung S-Y, Kim Y-M, Kim J-G, Kim Y-J. Multiphase transformation and Ostwald's rule of stages during crystallization of a metal phosphate. *Nat Phys*. 2009;5:68–73.
49. Rathje W. The formation of hydroxyfluor-apatite in tooth enamel under influence of drinking water containing fluoride. *J Dent Res*. 1952;31(6):761–766.
50. Bassett H. LVI.—The phosphates of calcium. Part IV. The basic phosphates. *J Chem Soc Trans*. 1917;111:620–642.
51. Narasaraaju TSB, Phebe DE. Some physico-chemical aspects of hydroxylapatite. *J Mater Sci*. 1996;31(1):1–21.
52. Collins R, Nebergall W, Langer H. A study of the reactions of various tin (II) compounds with calcium hydroxylapatite. *J Am Chem Soc*. 1961;83(17):3724–3725.
53. Meyer JL, Eanes ED. A thermodynamic analysis of the amorphous to crystalline calcium phosphate transformation. *Calcif Tissue Res*. 1978;25(1):59–68.
54. McConnell D. Crystal chemistry of hydroxyapatite: Its relation to bone mineral. *Arch Oral Biol*. 1965;10(3):421–431. doi:10.1016/0003-9969(65)90107-X
55. Narasaraaju TSB, Singh RP, Rao VLN. A new method of preparation of solid solutions of calcium and lead hydroxylapatites. *J Inorg Nucl Chem*. 1972;34(6):2072–2074.

56. Arnold PW. The nature of precipitated calcium phosphates. *Trans Faraday Soc.* 1950;46:1061–1072.
57. Narasraju TSB, Rao KK, Rai US, Kapoor BK. Preparation, characterization & solubility of arsenic hydroxylapatite; 1977.
58. Korber F, Trömel GZ. The formation of HAP through a solid state reaction between tri and tetra-calcium phosphates. *J Electrochem Soc.* 1932;38:578–580.
59. Tsigdinos GA. Heteropoly compounds of molybdenum and tungsten. In: *Topics in Current Chemistry*. Springer; 1978: 1–64.
60. Hayek E, Stadlmann W. Darstellung von reinem Hydroxylapatit für Adsorptionszwecke. *Angew Chemie.* 1955;67(12):327.
61. Main RK, Wilkins MJ, Cole LJ. A modified calcium phosphate for column chromatography of polynucleotides and proteins. *J Am Chem Soc.* 1959;81(24):6490–6495.
62. Cengiz B, Gokce Y, Yildiz N, Aktas Z, Calimli A. Synthesis and characterization of hydroxyapatite nanoparticles. *Colloids Surfaces a Physicochem Eng Asp.* 2008;322:29–33.
63. Antonakos A, Liarokapis E, Leventouri T. Micro-Raman and FTIR studies of synthetic and natural apatites. *Biomaterials.* 2007;28:3043–3054.
64. Nathanael AJ, Hong SI, Mangalaraj D, Ponpandian N, Chen PC. Template-free growth of novel hydroxyapatite nanorings: formation mechanism and their enhanced functional properties. *Cryst Growth Des.* 2012;12:3565–3574.
65. Kalita SJ, Verma S. Nanocrystalline hydroxyapatite bioceramic using microwave radiation: synthesis and characterization. *Mater Sci Eng C.* 2010;30:295–303.
66. Lu HB, Campbell CT, Graham DJ, Ratner BD. Surface characterization of hydroxyapatite and related calcium phosphates by XPS and TOF-SIMS. *Anal Chem.* 2000;72:2886–2894.
67. Munir MU, Ihsan A, Javed I, et al. Controllably biodegradable hydroxyapatite nanostructures for cefazolin delivery against antibacterial resistance. *ACS Omega.* 2019;4(4):7524–7532.
68. Yang Y-H, Liu C-H, Liang Y-H, Lin F-H, Wu KC-W. Hollow mesoporous hydroxyapatite nanoparticles (hmHANPs) with enhanced drug loading and pH-responsive release properties for intracellular drug delivery. *J Mater Chem B.* 2013;1:2447–2450.
69. Cao MH, Wang YH, Guo CX, Qi YJ, Hu CW. Preparation of ultrahigh-aspect-ratio hydroxyapatite nanofibers in reverse micelles under hydrothermal conditions. *Langmuir.* 2004;20(11):4784–4786.
70. Lee W-H, Loo C-Y, Rohanizadeh R. Functionalizing the surface of hydroxyapatite drug carrier with carboxylic acid groups to modulate the loading and release of curcumin nanoparticles. *Mater Sci Eng C.* 2019;99:929–939.
71. Zhou J, Horev B, Hwang G, Klein MI, Koo H, Benoit DSW. Characterization and optimization of pH-responsive polymer nanoparticles for drug delivery to oral biofilms. *J Mater Chem B.* 2016;4:3075–3085.
72. Haider A, Haider S, Han SS, Kang I-K. Recent advances in the synthesis, functionalization and biomedical applications of hydroxyapatite: a review. *Rsc Adv.* 2017;7:7442–7458.
73. Chen X, Fan H, Deng X, et al. Scaffold structural microenvironmental cues to guide tissue regeneration in bone tissue applications. *Nanomaterials.* 2018;8:960.
74. Hakobyan S, Roohpour N, Gautrot JE. Modes of adsorption of polyelectrolytes to model substrates of hydroxyapatite. *J Colloid Interface Sci.* 2019;543:237–246.
75. Pang S, Li X, Wu D, Li H, Wang X. Tuning inflammation response via adjusting microstructure of hydroxyapatite and biomolecules modification. *Colloids Surfaces B Biointerfaces.* 2019;177:496–505.
76. Tanaka H, Watanabe T, Chikazawa M, Kandori K, Ishikawa T. TPD, FTIR, and molecular adsorption studies of calcium hydroxyapatite surface modified with hexanoic and decanoic acids. *J Colloid Interface Sci.* 1999;214:31–37.
77. Tanaka H, Futaoka M, Hino R, Kandori K, Ishikawa T. Structure of synthetic calcium hydroxyapatite particles modified with pyrophosphoric acid. *J Colloid Interface Sci.* 2005;283:609–612.
78. Maurin AC, Chavassieux PM, Vericel E, Meunier PJ. Role of polyunsaturated fatty acids in the inhibitory effect of human adipocytes on osteoblastic proliferation. *Bone.* 2002;31:260–266.
79. Kim H. Biomedical nanocomposites of hydroxyapatite/polycaprolactone obtained by surfactant mediation. *J Biomed Mater Res Part a an off J Soc Biomater Japanese Soc Biomater Aust Soc Biomater Korean Soc Biomater.* 2007;83:169–177.
80. Williams JG. Polymeric materials encyclopedia. *J Am Chem Soc.* 1998;120(27):6848–6849.
81. Haider S, Park S-Y, Saeed K, Farmer BL. Swelling and electroresponsive characteristics of gelatin immobilized onto multi-walled carbon nanotubes. *Sensors Actuators B Chem.* 2007;124:517–528.
82. Dupraz AMP, De Wijn JR, Vd Meer SAT, De GK. Characterization of silane-treated hydroxyapatite powders for use as filler in biodegradable composites. *J Biomed Mater Res an off J Soc Biomater Japanese Soc Biomater.* 1996;30:231–238.
83. Zhao J-L, Fu T, Han Y, Xu K-W. Reinforcing hydroxyapatite/thermosetting epoxy composite with 3-D carbon fiber fabric through RTM processing. *Mater Lett.* 2004;58:163–168.
84. Santos C, Clarke RL, Braden M, Guitian F, Davy KWM. Water absorption characteristics of dental composites incorporating hydroxyapatite filler. *Biomaterials.* 2002;23:1897–1904.
85. Hong Z, Qiu X, Sun J, Deng M, Chen X, Jing X. Grafting polymerization of L-lactide on the surface of hydroxyapatite nano-crystals. *Polymer.* 2004;45:6699–6706.
86. Hong Z, Zhang P, He C, et al. Nano-composite of poly (L-lactide) and surface grafted hydroxyapatite: mechanical properties and biocompatibility. *Biomaterials.* 2005;26:6296–6304.
87. Gelse K, Pöschl E, Aigner T. Collagens—structure, function, and biosynthesis. *Adv Drug Deliv Rev.* 2003;55(12):1531–1546.
88. Della Bella E, Parrilli A, Bigi A, et al. Osteoinductivity of nanostructured hydroxyapatite-functionalized gelatin modulated by human and endogenous mesenchymal stromal cells. *J Biomed Mater Res Part A.* 2018;106(4):914–923.
89. Turco G, Marsich E, Bellomo F, et al. Alginate/hydroxyapatite biocomposite for bone ingrowth: a trabecular structure with high and isotropic connectivity. *Biomacromolecules.* 2009;10(6):1575–1583.
90. Cai X, Tong H, Shen X, Chen W, Yan J, Hu J. Preparation and characterization of homogeneous chitosan–polylactic acid/hydroxyapatite nanocomposite for bone tissue engineering and evaluation of its mechanical properties. *Acta Biomater.* 2009;5(7):2693–2703.
91. Silva SS, Duarte ARC, Oliveira JM, Mano JF, Reis RL. Alternative methodology for chitin–hydroxyapatite composites using ionic liquids and supercritical fluid technology. *J Bioact Compat Polym.* 2013;28(5):481–491.

92. Onoki T, Nakahira A, Tago T, Hasegawa Y, Kuno T. Novel low temperature processing techniques for apatite ceramics and chitosan polymer composite bulk materials and its mechanical properties. *Appl Surf Sci.* **2012**;262:263–266.
93. Kim H, Lee H, Knowles JC. Electrospinning biomedical nanocomposite fibers of hydroxyapatite/poly (lactic acid) for bone regeneration. *J Biomed Mater Res Part a an off J Soc Biomater Japanese Soc Biomater Aust Soc Biomater Korean Soc Biomater.* **2006**;79(3):643–649.
94. de Souza DC, de Oliveira PV, Capelo LP, Passos-Bueno MR, Catalani LH. A fast degrading PLLA composite with a high content of functionalized octacalcium phosphate mineral phase induces stem cells differentiation. *J Mech Behav Biomed Mater.* **2019**;93:93–104.
95. Ganesan K, Kovtun A, Neumann S, Heumann R, Epple M. Calcium phosphate nanoparticles: colloiddally stabilized and made fluorescent by a phosphate-functionalized porphyrin. *J Mater Chem.* **2008**;18(31):3655–3661.
96. Muddana HS, Morgan TT, Adair JH, Butler PJ. Photophysics of Cy3-encapsulated calcium phosphate nanoparticles. *Nano Lett.* **2009**;9(4):1559–1566.
97. Zhao C-X, Zhang W-D. Preparation of waterborne polyurethane nanocomposites: polymerization from functionalized hydroxyapatite. *Eur Polym J.* **2008**;44(7):1988–1995.
98. Sokolova VV, Radtke I, Heumann R, Epple M. Effective transfection of cells with multi-shell calcium phosphate-DNA nanoparticles. *Biomaterials.* **2006**;27(16):3147–3153.
99. Deshmukh K, Ramanan SR, Kowshik M. Novel one step transformation method for Escherichia coli and Staphylococcus aureus using arginine-glucose functionalized hydroxyapatite nanoparticles. *Mater Sci Eng C.* **2019**;96:58–65.
100. Sheikh I, Dahman Y. Applications of nanobiomaterials in hard tissue engineering. In: *Nanobiomaterials in Hard Tissue Engineering*. Elsevier; **2016**: 33–62.
101. Bang LT, Long BD, Othman R. Carbonate hydroxyapatite and silicon-substituted carbonate hydroxyapatite: synthesis, mechanical properties, and solubility evaluations. *Sci World J.* **2014**;2014:54.
102. Dahl SG, Allain P, Marie PJ, et al. Incorporation and distribution of strontium in bone. *Bone.* **2001**;28(4):446–453.
103. Ammann P. Strontium ranelate: a novel mode of action leading to renewed bone quality. *Osteoporos Int.* **2005**;16(1):S11–S15.
104. Capuccini C, Torricelli P, Boanini E, Gazzano M, Giardino R, Bigi A. Interaction of Sr-doped hydroxyapatite nanocrystals with osteoclast and osteoblast-like cells. *J Biomed Mater Res Part a an off J Soc Biomater Japanese Soc Biomater Aust Soc Biomater Korean Soc Biomater.* **2009**;89(3):594–600.
105. Zhao Z, Espanol M, Guillem-Marti J, Kempf D, Diez-Escudero A, Ginebra M-P. Ion-doping as a strategy to modulate hydroxyapatite nanoparticle internalization. *Nanoscale.* **2016**;8:1595–1607.
106. Bodhak S, Bose S, Bandyopadhyay A. Bone cell-material interactions on metal-ion doped polarized hydroxyapatite. *Mater Sci Eng C.* **2011**;31:755–761.
107. Li Y, Widodo J, Lim S, Ooi CP. Synthesis and cytocompatibility of manganese (II) and iron (III) substituted hydroxyapatite nanoparticles. *J Mater Sci.* **2012**;47:754–763.
108. Bose S, Fielding G, Tarafder S, Bandyopadhyay A. Understanding of dopant-induced osteogenesis and angiogenesis in calcium phosphate ceramics. *Trends Biotechnol.* **2013**;31:594–605.
109. Medvecký L, Štulajterová R, Parilák L, Trpčevská J, Ďurišin J, Barinov SM. Influence of manganese on stability and particle growth of hydroxyapatite in simulated body fluid. *Colloids Surfaces a Physicochem Eng Asp.* **2006**;281(1–3):221–229.
110. Rico H, Gomez-Raso N, Revilla M, et al. Effects on bone loss of manganese alone or with copper supplement in ovariectomized rats: a morphometric and densitometric study. *Eur J Obstet Gynecol Reprod Biol.* **2000**;90(1):97–101.
111. Mayer I, Jacobsohn O, Niazov T, et al. Manganese in precipitated hydroxyapatites. *Eur J Inorg Chem.* **2003**;2003(7):1445–1451.
112. Kawasaki T, Takahashi S, Iweda K. Hydroxyapatite high-performance liquid chromatography: column performance for proteins. *Eur J Biochem.* **1985**;152:361–371.
113. Munir MU, Ahmad MM. Nanomaterials aiming to tackle antibiotic-resistant bacteria. *Pharmaceutics.* **2022**;14(3):582.
114. Zhang S. *Hydroxyapatite Coatings for Biomedical Applications*. CRC press; **2013**.
115. Chen X, Wang Q, Shen J, Pan H, Wu T. Adsorption of leucine-rich amelogenin protein on hydroxyapatite (001) surface through COO-Claws. *J Phys Chem C.* **2007**;111:1284–1290.
116. Shaw WJ, Campbell AA, Paine ML, Snead ML. The COOH terminus of the amelogenin, LRAP, is oriented next to the hydroxyapatite surface. *J Biol Chem.* **2004**;279:40263–40266.
117. Kandori K, Oda S, Fukusumi M, Morisada Y. Synthesis of positively charged calcium hydroxyapatite nano-crystals and their adsorption behavior of proteins. *Colloids Surfaces B Biointerfaces.* **2009**;73:140–145.
118. Qi C, Musetti S, Fu L-H, Zhu Y-J HL. Biomolecule-assisted green synthesis of nanostructured calcium phosphates and their biomedical applications. *Chem Soc Rev.* **2019**;48:2698–2737.
119. Munir A, Muhammad F, Zaheer Y, et al. Synthesis of naringenin loaded lipid based nanocarriers and their in-vivo therapeutic potential in a rheumatoid arthritis model. *J Drug Deliv Sci Technol.* **2021**;66. doi:10.1016/j.jddst.2021.102854
120. Deshmukh K, Ramanan SR, Kowshik M. A novel method for genetic transformation of C. albicans using modified-hydroxyapatite nanoparticles as a plasmid DNA vehicle. *Nanoscale Adv.* **2019**;1:3015–3022.
121. Tram DTN, Lee W-H, Loo C-Y, Zavgorodniy AV, Rohanizadeh R. Hydroxyapatite nanoparticles as vectors for gene delivery. *Ther Deliv.* **2012**;3:623–632.
122. Tan K, Cheang P, Ho IAW, Lam PYP, Hui KM. Nanosized bioceramic particles could function as efficient gene delivery vehicles with target specificity for the spleen. *Gene Ther.* **2007**;14:828–835.
123. Liu H, Chen F, Xi P, et al. Biocompatible fluorescent hydroxyapatite: synthesis and live cell imaging applications. *J Phys Chem C.* **2011**;115:18538–18544.
124. Deshmukh K, Shaik MM, Ramanan SR, Kowshik M. Self-activated fluorescent hydroxyapatite nanoparticles: a promising agent for bioimaging and biolabeling. *ACS Biomater Sci Eng.* **2016**;2:1257–1264.
125. Hao X, Hu X, Zhang C, et al. Hybrid mesoporous silica-based drug carrier nanostructures with improved degradability by hydroxyapatite. *ACS Nano.* **2015**;9(10):9614–9625.
126. Munir MU, Salman S, Javed I, et al. Nano-hydroxyapatite as a delivery system; overview and advancements. *Artif Cells, Nanomed, Biotechnol.* **2021**. doi:10.1080/21691401.2021.2016785

127. Yu J, Chu X, Cai Y, Tong P, Yao J. Preparation and characterization of antimicrobial nano-hydroxyapatite composites. *Mater Sci Eng C*. 2014;37:54–59.
128. Lian X, Liu H, Wang X, Xu S, Cui F, Bai X. Antibacterial and biocompatible properties of vancomycin-loaded nano-hydroxyapatite/collagen/poly (lactic acid) bone substitute. *Prog Nat Sci Mater Int*. 2013;23(6):549–556.
129. Palazzo B, Iafisco M, Laforgia M, et al. Biomimetic hydroxyapatite–drug nanocrystals as potential bone substitutes with antitumor drug delivery properties. *Adv Funct Mater*. 2007;17(13):2180–2188.
130. Kirkham J, Brookes SJ, Shore RC, et al. Physico-chemical properties of crystal surfaces in matrix–mineral interactions during mammalian biomineralisation. *Curr Opin Colloid Interface Sci*. 2002;7:124–132.
131. Rimola A, Corno M, Zicovich-Wilson CM, Ugliengo P. Ab initio modeling of protein/biomaterial interactions: glycine adsorption at hydroxyapatite surfaces. *J Am Chem Soc*. 2008;130:16181–16183.
132. Yewle JN, Wei Y, Puleo DA, Daunert S, Bachas LG. Oriented immobilization of proteins on hydroxyapatite surface using bifunctional bisphosphonates as linkers. *Biomacromolecules*. 2012;13:1742–1749.
133. Li Z, Liu Z, Yin M, et al. Aptamer-capped multifunctional mesoporous strontium hydroxyapatite nanovehicle for cancer-cell-responsive drug delivery and imaging. *Biomacromolecules*. 2012;13:4257–4263.
134. Son JS, Choi Y, Park E, Kwon T, Kim K, Lee K. Drug delivery from hydroxyapatite-coated titanium surfaces using biodegradable particle carriers. *J Biomed Mater Res Part B Appl Biomater*. 2013;101:247–257.
135. Ibrahim A-R, Li X, Zhou Y, et al. Synthesis of spongy-like mesoporous hydroxyapatite from raw waste eggshells for enhanced dissolution of ibuprofen loaded via supercritical CO₂. *Int J Mol Sci*. 2015;16:7960–7975.
136. Koocheki S, Madaeni SS, Niroomandi P. Application of hydroxyapatite nanoparticles in development of an enhanced formulation for delivering sustained release of triamcinolone acetonide. *Int J Nanomedicine*. 2011;6:825.
137. Loo SCJ, Moore T, Banik B, Alexis F. Biomedical applications of hydroxyapatite nanoparticles. *Curr Pharm Biotechnol*. 2010;11:333–342.
138. Fan Q, Wang YE, Zhao X, Loo JSC, Zuo YY. Adverse biophysical effects of hydroxyapatite nanoparticles on natural pulmonary surfactant. *ACS Nano*. 2011;5:6410–6416.
139. Hetrick EM, Schoenfish MH. Reducing implant-related infections: active release strategies. *Chem Soc Rev*. 2006;35:780–789.
140. Pishbin F, Mourão V, Flor S, et al. Electrophoretic deposition of gentamicin-loaded bioactive glass/chitosan composite coatings for orthopaedic implants. *ACS Appl Mater Interfaces*. 2014;6:8796–8806.
141. Raphael J, Holodniy M, Goodman SB, Heilshorn SC. Multifunctional coatings to simultaneously promote osseointegration and prevent infection of orthopaedic implants. *Biomaterials*. 2016;84:301–314.
142. Nasiri N, Mukherjee S, Panneerselvam A, Nisbet DR, Tricoli A. Optimally hierarchical nanostructured hydroxyapatite coatings for superior prosthesis biointegration. *ACS Appl Mater Interfaces*. 2018;10(29):24840–24849.
143. Asri RIM, Harun WSW, Hassan MA, Ghani SAC, Buyong Z. A review of hydroxyapatite-based coating techniques: sol–gel and electrochemical depositions on biocompatible metals. *J Mech Behav Biomed Mater*. 2016;57:95–108.
144. Daugaard H, Elmengaard B, Bechtold JE, Jensen T, Soballe K. The effect on bone growth enhancement of implant coatings with hydroxyapatite and collagen deposited electrochemically and by plasma spray. *J Biomed Mater Res Part a an off J Soc Biomater Japanese Soc Biomater Aust Soc Biomater Korean Soc Biomater*. 2010;92(3):913–921.
145. Yu JC, Ho W, Lin J, Yip H, Wong PK. Photocatalytic activity, antibacterial effect, and photoinduced hydrophilicity of TiO₂ films coated on a stainless steel substrate. *Environ Sci Technol*. 2003;37:2296–2301.
146. Tobin EJ. Recent coating developments for combination devices in orthopedic and dental applications: a literature review. *Adv Drug Deliv Rev*. 2017;112:88–100.
147. Geesink RG, de Groot K, Klein CP. Bonding of bone to apatite-coated implants. *J Bone Joint Surg Br*. 1988;70:17–22.
148. Zagayva T, Balázsi K, Balázsi C. Examination of novel electrosprayed biogenic hydroxyapatite coatings on Si₃N₄ and Si₃N₄/MWCNT ceramic composite. *Process Appl Ceram*. 2019;13(2):132–138.
149. Tian H, Tang Z, Zhuang X, Chen X, Jing X. Biodegradable synthetic polymers: preparation, functionalization and biomedical application. *Prog Polym Sci*. 2012;37:237–280.
150. de Siqueira L, Ribeiro N, Paredes M, et al. Influence of PLLA/PCL/HA scaffold fiber orientation on mechanical properties and osteoblast behavior. *Materials (Basel)*. 2019;12(23):3879.
151. LeGeros RZ. Properties of osteoconductive biomaterials: calcium phosphates. *Clin Orthop Relat Res*. 2002;395:81–98.
152. Liang H, Liu X, Pi Y, et al. 3D-printed β -tricalcium phosphate scaffold combined with a pulse electromagnetic field promotes the repair of skull defects in rats. *ACS Biomater Sci Eng*. 2019;5:5359–5367.
153. Guo B, Ma PX. Synthetic biodegradable functional polymers for tissue engineering: a brief review. *Sci China Chem*. 2014;57:490–500.
154. Guo B, Ma PX. Conducting polymers for tissue engineering. *Biomacromolecules*. 2018;19:1764–1782.
155. Sell SA, Wolfe PS, Garg K, McCool JM, Rodriguez IA, Bowlin GL. The use of natural polymers in tissue engineering: a focus on electrospun extracellular matrix analogues. *Polymers*. 2010;2:522–553.
156. Urist MR. Bone: formation by autoinduction. *Science (80-)*. 1965;150:893–899.
157. Kulkarni RK, Moore EG, Hegyeli AF, Leonard F. Biodegradable poly (lactic acid) polymers. *J Biomed Mater Res*. 1971;5:169–181.
158. Zhao J, Guo LY, Yang XB, Weng J. Preparation of bioactive porous HA/PCL composite scaffolds. *Appl Surf Sci*. 2008;255:2942–2946.
159. Higashi S, Yamamuro T, Nakamura T, Ikada Y, Hyon S-H, Jamshidi K. Polymer-hydroxyapatite composites for biodegradable bone fillers. *Biomaterials*. 1986;7:183–187.
160. Park J-W, Hwang J-U, Back J-H, et al. High strength PLGA/Hydroxyapatite composites with tunable surface structure using PLGA direct grafting method for orthopedic implants. *Compos Part B Eng*. 2019;178:107449.
161. Bose S, Dasgupta S, Tarafder S, Bandyopadhyay A. Microwave-processed nanocrystalline hydroxyapatite: simultaneous enhancement of mechanical and biological properties. *Acta Biomater*. 2010;6:3782–3790.
162. Ahmed A, Sarwar S, Hu Y, et al. Surface-modified polymeric nanoparticles for drug delivery to cancer cells. *Expert Opin Drug Deliv*. 2021;18(1). doi:10.1080/17425247.2020.1822321
163. Shin Y-S, Borah JS, Haider A, Kim S, Huh M-W, Kang I-K. Fabrication of pamidronic acid-immobilized TiO₂/hydroxyapatite composite nanofiber mats for biomedical applications. *J Nanomater*. 2013;2013:e34.

164. Ignjatovic N, Delijic K, Vukcevic M, Uskokovic D. The designing of properties of hydroxyapatite/poly-L-lactide composite biomaterials by hot pressing. *Zeitschrift fur Met.* **2001**;92:145–149.
165. Wang M, Joseph R, Bonfield W. Hydroxyapatite-polyethylene composites for bone substitution: effects of ceramic particle size and morphology. *Biomaterials.* **1998**;19:2357–2366.
166. Dalby MJ, Di Silvio L, Harper EJ, Bonfield W. In vitro evaluation of a new polymethylmethacrylate cement reinforced with hydroxyapatite. *J Mater Sci Mater Med.* **1999**;10:793–796.
167. Orlovskii VP, Komlev VS, Barinov SM. Hydroxyapatite and hydroxyapatite-based ceramics. *Inorg Mater.* **2002**;38:973–984.
168. Ronan K, Kannan MB. Novel sustainable route for synthesis of hydroxyapatite biomaterial from biowastes. *ACS Sustain Chem Eng.* **2017**;5:2237–2245.
169. Chesnutt BM, Viano AM, Yuan Y, et al. Design and characterization of a novel chitosan/nanocrystalline calcium phosphate composite scaffold for bone regeneration. *J Biomed Mater Res Part A.* **2009**;88:491–502.
170. Zhang W, Liao SS, Cui FZ. Hierarchical self-assembly of nano-fibrils in mineralized collagen. *Chem Mater.* **2003**;15:3221–3226.
171. Rhee S, Do LJ, Tanaka J. Nucleation of hydroxyapatite crystal through chemical interaction with collagen. *J Am Ceram Soc.* **2000**;83:2890–2892.
172. Li B, Kan L, Zhang X, et al. Biomimetic bone-like hydroxyapatite by mineralization on supramolecular porous fiber networks. *Langmuir.* **2017**;33:8493–8502.
173. Kalita SJ, Bose S, Hosick HL, Bandyopadhyay A. CaO–P₂O₅–Na₂O-based sintering additives for hydroxyapatite (HAp) ceramics. *Biomaterials.* **2004**;25:2331–2339.
174. Huang B, Caetano G, Vyas C, Blaker JJ, Diver C, Bártolo P. Polymer-ceramic composite scaffolds: the effect of hydroxyapatite and β -tri-calcium phosphate. *Materials (Basel).* **2018**;11:129.
175. Fang J, Li P, Lu X, Fang L, Lü X, Ren F. A strong, tough, and osteoconductive hydroxyapatite mineralized polyacrylamide/dextran hydrogel for bone tissue regeneration. *Acta Biomater.* **2019**;88:503–513.
176. Shi C, Gao J, Wang M, et al. Functional hydroxyapatite bioceramics with excellent osteoconductivity and stern-interface induced antibacterial ability. *Biomater Sci.* **2016**;4:699–710.
177. Vincent J. *Structural Biomaterials*. Princeton University Press; **2012**.
178. Zhao C, Wang X, Gao L, Jing L, Zhou Q, Chang J. The role of the micro-pattern and nano-topography of hydroxyapatite bioceramics on stimulating osteogenic differentiation of mesenchymal stem cells. *Acta Biomater.* **2018**;73:509–521.
179. Yang C, Zhao C, Wang X, et al. Stimulation of osteogenesis and angiogenesis by micro/nano hierarchical hydroxyapatite via macrophage immunomodulation. *Nanoscale.* **2019**;11(38):17699–17708.
180. Ruys AJ, Wei M, Sorrell CC, Dickson MR, Brandwood A, Milthorpe BK. Sintering effects on the strength of hydroxyapatite. *Biomaterials.* **1995**;16:409–415.
181. Mostafa NY. Characterization, thermal stability and sintering of hydroxyapatite powders prepared by different routes. *Mater Chem Phys.* **2005**;94:333–341.
182. Uchida A, Shinto Y, Araki N, Ono K. Slow release of anticancer drugs from porous calcium hydroxyapatite ceramic. *J Orthop Res.* **1992**;10:440–445.
183. Liu D-M. Preparation and characterisation of porous hydroxyapatite bioceramic via a slip-casting route. *Ceram Int.* **1998**;24:441–446.
184. Quinlan E, López-Noriega A, Thompson EM, Hibbitts A, Cryan SA, O'Brien FJ. Controlled release of vascular endothelial growth factor from spray-dried alginate microparticles in collagen-hydroxyapatite scaffolds for promoting vascularization and bone repair. *J Tissue Eng Regen Med.* **2017**;11:1097–1109.
185. Casarrubios L, Gómez-Cerezo N, Sánchez-Salcedo S, et al. Silicon substituted hydroxyapatite/VEGF scaffolds stimulate bone regeneration in osteoporotic sheep. *Acta Biomater.* **2020**;101:544–553.
186. Ahn ES, Gleason NJ, Nakahira A, Ying JY. Nanostructure processing of hydroxyapatite-based bioceramics. *Nano Lett.* **2001**;1:149–153.
187. Phipps MC, Clem WC, Grunda JM, Clines GA, Bellis SL. Increasing the pore sizes of bone-mimetic electrospun scaffolds comprised of polycaprolactone, collagen I and hydroxyapatite to enhance cell infiltration. *Biomaterials.* **2012**;33:524–534.
188. Watson KE, Tenhuisen KS, Brown PW. The formation of hydroxyapatite–calcium polyacrylate composites. *J Mater Sci Mater Med.* **1999**;10:205–213.
189. Moseke C, Gbureck U. Tetracalcium phosphate: synthesis, properties and biomedical applications. *Acta Biomater.* **2010**;6:3815–3823.
190. Knepper M, Moricca S, Milthorpe BK. Stability of hydroxyapatite while processing short-fibre reinforced hydroxyapatite ceramics. *Biomaterials.* **1997**;18:1523–1529.
191. Shikami Y, Okuno M. Bioresorbable devices made of forged composites of hydroxyapatite (HA) particles and poly L-lactide (PLLA). Part II: practical properties of miniscrews and miniplates. *Biomaterials.* **2001**;22:3197–3211.
192. Yoshikawa H, Tamai N, Murase T, Myoui A. Interconnected porous hydroxyapatite ceramics for bone tissue engineering. *J R Soc Interface.* **2009**;6(suppl_3):S341–S348.
193. Munir MU, Ahmed A, Usman M, Salman S. Recent advances in nanotechnology-aided materials in combating microbial resistance and functioning as antibiotics substitutes. *Int J Nanomedicine.* **2020**;15:7329.